GLUING KARCHER–SCHERK SADDLE TOWERS I: TRIPLY PERIODIC MINIMAL SURFACES

HAO CHEN AND MARTIN TRAIZET

ABSTRACT. We construct minimal surfaces by gluing simply periodic Karcher–Scherk saddle towers along their wings. Such constructions were previously implemented assuming a horizontal reflection plane. We break this symmetry by prescribing phase differences between the saddle towers. It turns out that, in addition to the previously known horizontal balancing condition, the saddle towers must also be balanced under a subtle vertical interaction. This interaction vanishes in the presence of a horizontal reflection plane, hence was not perceived in previous works.

Our construction will be presented in a series of papers. In this first paper of the series, we will explain the background of the project and establish the graph theoretical setup that will be useful for all papers in the series. The main task of the current paper is to glue saddle towers into triply periodic minimal surfaces (TPMSs). Our construction expands many previously known TPMSs into new 5-parameter families, therefore significantly advances our knowledge on the space of TPMSs.

1. BACKGROUND

In the last decades, the node-opening technique has been very successful in gluing catenoids into minimal surfaces of finite or infinite topology in Euclidean space forms [Tra02b, Tra02a, Tra08, MT12, CT21].

In fact, the technique was first developed to glue Karcher–Scherk saddle towers. More specifically, the second named author desingularized arrangements of vertical planes into minimal surfaces by replacing the intersection lines with Scherk surfaces (saddle towers with four wings). This was first done by solving non-linear PDEs [Tra96] and later using the node-opening technique [Tra01]. In his thesis [You09], Rami Younes desingularized $\mathsf{G} \times \mathbb{R}$, where G is a graph embedded in a flat 2-torus, into triply periodic minimal surfaces by placing saddle towers over the vertices of G. These constructions work only when all saddle towers are balanced under a horizontal interaction or, equivalently, when the graph embedding is a non-degenerate critical point of the length functional.

All these previous works assumed, however, that the surfaces have a horizontal reflection plane. It was wondered in [Tra96] whether this symmetry is necessary for simply periodic minimal surfaces (SPMSs) with ends of Scherk type (i.e. asymptotic to vertical planes). A positive answer was given for SPMSs of genus 0 [PT07], but Martín and Ramos Batista constructed the Karcher–Costa towers [MRB06] that provide examples of genus 1 without horizontal symmetry. The same question can

be asked for triply periodic minimal surfaces (TPMSs). But the deformation families of the Gyroid, which were recently confirmed by the first named author [Che21] admit saddle tower limits but do not have any horizontal symmetry plane (see Figure 1).
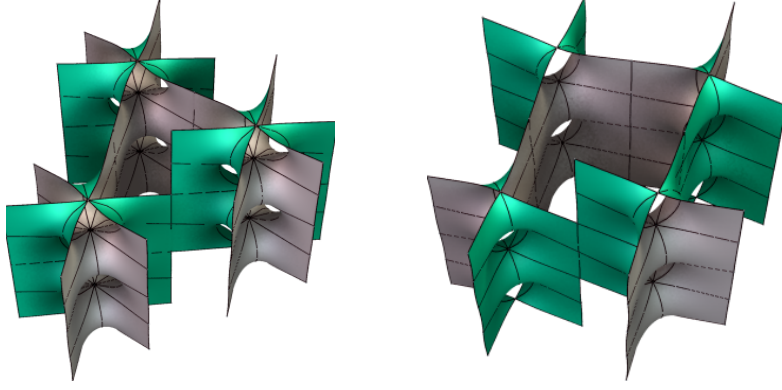

FIGURE 1. A rhombohedral (left) and a tetragonal (right) deformation of the Gyroid near the saddle tower limits. They do not have any horizontal symmetry plane.

The goal of this series of papers is to glue Karcher–Scherk saddle towers into minimal surfaces, without the assumption of a horizontal reflection plane.

Let G be a graph in the complex plane. Formal definitions will be given in Section 3. At the moment, it suffices to understand that G is a set of straight segments (edges) and half-lines (rays) that intersect only at their endpoints (vertices). There are different possible setups, depending on weather the graph G is finite, periodic with finite quotient, or infinite aperiodic.

For sufficiently small $\varepsilon > 0$, we want to construct a 1-parameter family $(\mathscr{M}_\varepsilon)_{\varepsilon > 0}$ of embedded minimal surfaces of vertical period $2\pi\varepsilon^2$ that tends to $\mathsf{G} \times \mathbb{R}$ as $\varepsilon \to 0$. For this purpose, we place suitably scaled saddle towers over the vertices of G and glue their wings along the edges of the graph.

Since the fluxes along the wings of a saddle tower sum up to 0, the graph G must be balanced in the sense that for each vertex v, the sum of the unit vectors in the directions of the outgoing edges adjacent to v is zero. We call the sum the horizontal force.

Orientability of $\mathscr{M}_\varepsilon$ requires the graph G to be orientable, in the sense that its faces can be labelled with $+$ or $-$ signs so that adjacent faces have opposite signs. The prototype result in the symmetric case is the following:

Theorem 1.1 (Informal statement). *Let G be a balanced, rigid and orientable graph. Then $\mathsf{G} \times \mathbb{R}$ can be desingularized into a family of minimal surfaces $\mathscr{M}_\varepsilon$ that have vertical period $2\pi\varepsilon^2$ and are symmetric with respect to a horizontal plane.*

Rigidity concerns the invertibility of the Jacobian of horizontal forces. Its precise formulation depends on the setup under consideration.

Theorem 1.1 was first proved in [Tra01] when G appears as a line arrangement, yielding a family of SPMSs with Scherk-type ends. It was then proved in [You09] when G is a doubly-periodic graph with finite quotient, yielding a family of TPMSs. See Theorem 4.9 for a precise statement in this case.

To break the horizontal symmetry, we must move the saddle towers vertically so that they have different reflection planes. The "height differences" between the

reflection planes, known as the phase differences, are prescribed on the edges of the graph.

Technically, the phase differences correspond to the complex arguments of the node-opening parameters; see Section 8.1 for details. Complex node-opening parameters were considered in previous works [Tra08], but never did the complex argument play such an important role.

This paper reveals that the phase differences must satisfy a balancing condition, known as vertical balancing, which is more subtle and delicate than horizontal balancing of the graph G. The formulation of vertical balancing requires quite a lot of preliminaries, but we can give an idea of what it looks like.

Assume that two saddle towers $\mathscr{S}$ and $\mathscr{S}'$ are glued along their wings. Let ℓ be the length of the corresponding edge in the graph, and ϕ be the prescribed phase difference of $\mathscr{S}'$ over $\mathscr{S}$. Then, as $\varepsilon \to 0$, the vertical force exerted by $\mathscr{S}'$ on $\mathscr{S}$ is asymptotically of the form

$$K \sin(\phi) \exp(-\ell/\varepsilon^2).$$

where the coefficient K is a positive real number that depends on the undulation of the saddle towers and a first-order deformation of the graph. Because of the factor $\sin(\phi)$, the force vanishes whenever $\phi = 0$ or π. This explains why this interaction was not perceived in previous works that assumed a reflection symmetry.

The vertical balancing condition requires, for every set of saddle towers, that the forces sum up to 0 over the edges that separate the set from other saddle towers. Because of the exponential factor, the interaction dominates on shorter edges of the graph for small ε. So in the limit $\varepsilon \to 0$, it suffices to take the sum of $K \sin(\phi)$ over the shortest separating edges.

The prototype result in the non-symmetric case is the following:

Theorem 1.2 (Informal statement)**.** *Let G be a balanced, rigid and orientable graph with phase differences ϕ prescribed on the edges. Assume that ϕ is balanced and rigid. Then $\mathsf{G} \times \mathbb{R}$ can be desingularized into a family of minimal surfaces $\mathscr{M}_\varepsilon$ which have vertical period $2\pi\varepsilon^2$. Moreover, for each vertex v, $\varepsilon^{-2}\mathscr{M}_\varepsilon$ converges after suitable horizontal translation to a saddle tower $\mathscr{S}_v$, and the phase differences between adjacent saddle towers are given by ϕ.*

Rigidity of ϕ concerns the invertibility of the Jacobian of vertical forces. Again, its precise formulation depends on the given setup.

The goal of this first paper in the series is to prove Theorem 1.2 when G is a doubly-periodic graph with finite quotient, resulting in TPMSs. See Theorem 6.7 for the precise formulation of our main result. TPMSs are given the privilege because many known families of TPMSs admit saddle tower limits, but most of them are symmetric in a horizontal plane; see Figure 2. So we expect to find many interesting new examples after breaking this symmetry.

The paper is organized as follows.

In Section 2, we recall some basic facts about Karcher–Scherk saddle towers and give a geometric definition of phases. Section 3 sets up the graph theoretical foundation, which is crucial for formal statements of the main results. Then in Section 4, we define horizontal balance and rigidity, and recall Younes' result about symmetric TPMSs.

Section 5 is dedicated to an in-depth investigation on the shapes of the wings. We will define new quantities in terms of Weierstrass data. They will be useful in Section 6 for defining vertical balance and rigidity, and for announcing our main Theorem 6.7 about non-symmetric TPMSs. Then we present in Section 7 examples

(a) oPa   (b) oPb   (c) oCLP

(d) H   (e) oH   (f) H'–T

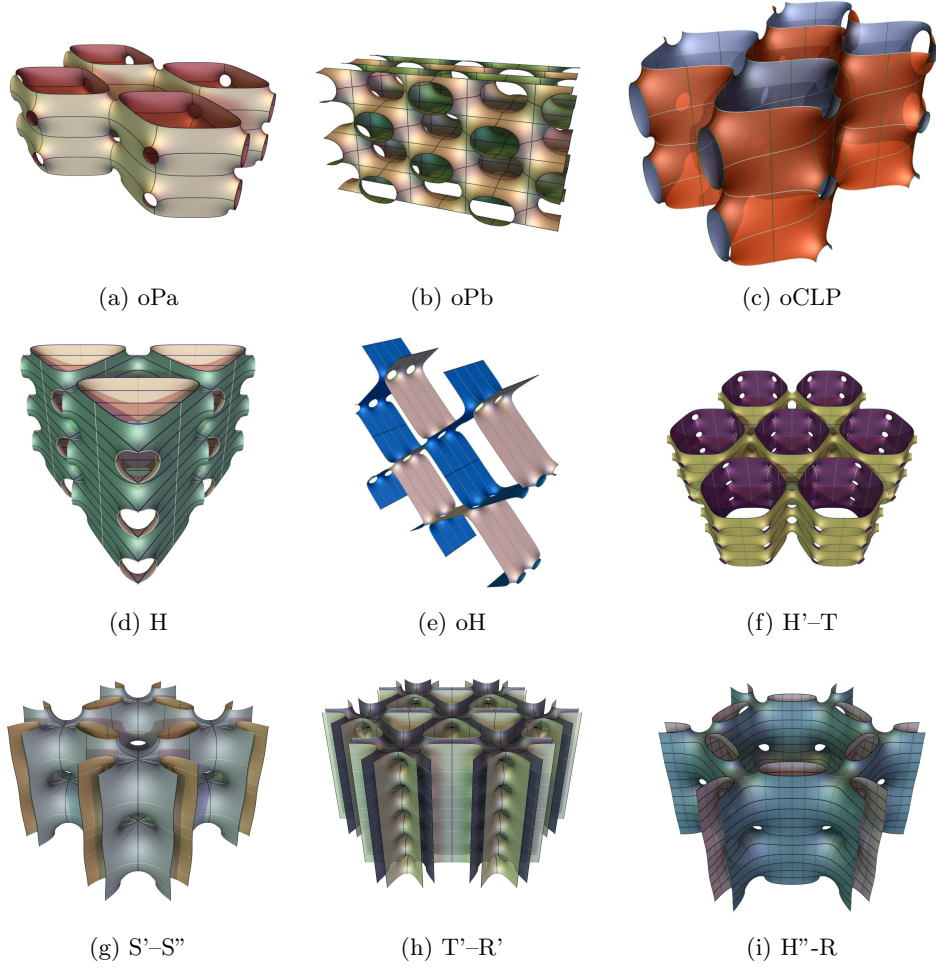(g) S'–S"   (h) T'–R'   (i) H"-R

FIGURE 2. A gallery of known examples of saddle tower limits of triply periodic minimal surfaces (Source: Matthias Weber). Generalizations of them will be constructed in this paper.

of TPMSs that can be produced from our construction, including many new TPMSs of genus 3. The construction is finally proved in Section 8.

Note that the sections 2, 3, 5 are preparatory, meant to be relevant not only for the current manuscript but also for future papers.

Acknowledgement. The authors thank Matthias Weber for an unbelievable video of triply periodic minimal surfaces that motivated this project.

2. First look on Karcher–Scherk saddle towers

Recall that a *saddle tower* is an embedded SPMS with n Scherk-type ends, where $n \geq 4$ is an even integer. Saddle towers with $n = 4$ were discovered by Scherk [Sch35] in the 19th century. All other saddle towers were constructed by Karcher [Kar88]. Saddle towers are classified in [PT07] as the only embedded SPMS with n Scherk-type ends and genus zero in the quotient by the period.

We sketch Karcher's construction as follows: Let P be a convex polygon with n sides of length one, where $n \geq 4$ is even. We allow P to be non-strictly convex but exclude the *degenerate* case where P appears as a line segment of length $n/2$, and
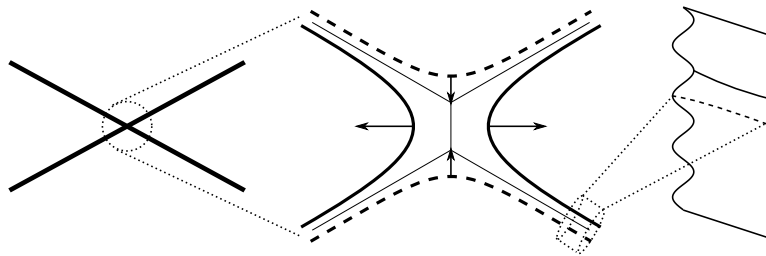
FIGURE 3. A four-wing saddle tower seen from a distance (left), then scaled at the "axis" (middle). The shape of a wing is illustrated on the right, featuring the undulation.

the *special* case where $n \geq 6$ and P appears as a parallelogram with 2 sides of length one [PT07]. Then the Jenkins–Serrin theorem [JS66] guarantees the existence of a minimal graph over the interior of P that takes the values $\pm\infty$, alternately, on the edges of P, unique up to vertical translation. This graph is bounded by vertical lines over the vertices of P. Its conjugate minimal surface is bounded by n curvature lines that lie, alternately, in two horizontal planes at distance 1 from each other. Reflections in these planes extend the conjugate surface into an SPMS called a saddle tower, which we denote by $\mathscr{S}$.

The edges of P are n unit vectors that sum up to 0. To be consistent with later notations, we label the edges by $\mathsf{H} = \{0, \cdots, n-1\}$ in the counterclockwise order, and define $\varsigma : \mathsf{H} \to \mathsf{H}$ by $\varsigma(h) = h + 1 \pmod{n}$. Let the corresponding unit vectors be $u_h = \exp(\mathrm{i}\theta_h) \in \mathbb{C} \simeq \mathbb{R}^2$, $h \in \mathsf{H}$. The corresponding ends of $\mathscr{S}$ are called *wings*. Each wing is asymptotic to a vertical half-plane that is parallel to the corresponding edge. Wings extending in the same direction (same θ_h) are called *parallel*.

We now make a distinction between the two horizontal reflection planes. Fix an orientation of $\mathscr{S}$. It is known that the conjugate minimal surface of the Jenkins–Serrin graph is a graph over an unbounded concave domain Ω. The complement of Ω has n unbounded convex components, each bounded by the projection of a curvature line (see [Kar88]). We say that a curvature line γ is a 0-arc if the Gauss map on γ points into the corresponding convex component. All 0-arcs lie on the same horizontal symmetry plane, which we call the 0-plane. We scale all our saddle towers so that their vertical period is 2π.

Definition 2.1 (Phase). Let $\mathscr{S}$ be an oriented saddle tower of vertical period 2π. We say that the *phase* of $\mathscr{S}$ is $\phi \in \mathbb{R}/2\pi\mathbb{Z}$ if the horizontal plane $x_3 = \phi$ is a 0-plane of $\mathscr{S}$.

Remark 2.2. Seen from a distance, $\mathscr{S}$ looks like n vertical half-planes sharing a vertical boundary; see Figure 3 (left). But a closer look reveals that the asymptotic planes of the wings do not intersect at a single vertical line; see Figure 3 (middle) for an illustration and Section 5.3.1 for a detailed analysis.

3. Graphs

Graph theory plays a central role in our construction. Combinatorially, we use a graph to describe how saddle towers (vertices) are glued along wings (edges) into a minimal surface. Geometrically, the degenerate limit of our surface projects to a horizontal plane as a geometric "representation" of the graph.
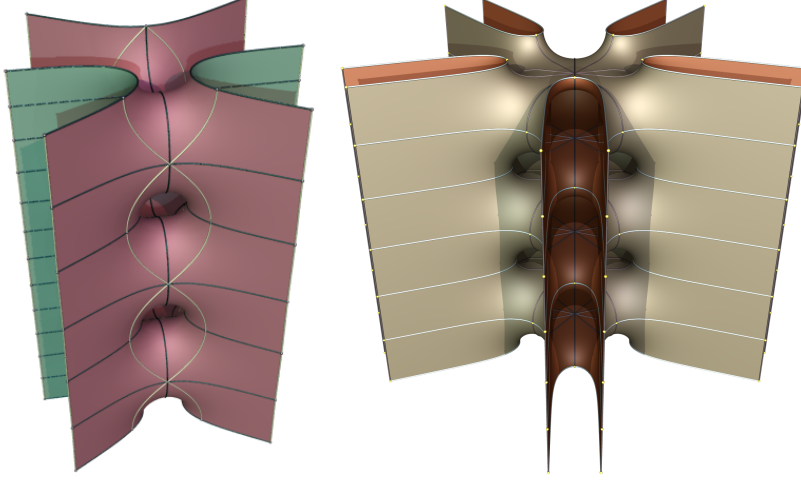
FIGURE 4. Two saddle towers with six and ten wings; see Section 5.3.
The one on the right has five pairs of parallel wings. (Source: Matthias
Weber)

In this paper, a "graph" actually refers to a multigraph, possibly with multiple
edges and loops. This maximizes the generality of our construction. Such a multi-
graph is best described in terms of rotation systems. The standard references for
this section are [GR01, MT01, Die17].

3.1. **Intuitive picture.** For readers not familiar with rotation systems, we give
here an intuitive picture which, although informal, should suffice for understanding
our construction.

A graph G in a flat 2-torus $\mathbb{T}^2$ can be understood as a set V of points (vertices) and
a set E of straight segments (edges) whose endpoints are (not necessarily distinct)
vertices and whose interiors are disjoint. The connected components of $\mathbb{T}^2 \setminus \mathsf{G}$ are
called faces. The set of faces is denoted F. By Euler formula,

$$|\mathsf{V}| - |\mathsf{E}| + |\mathsf{F}| = 0.$$

Each edge has two possible orientations, i.e. a choice of "initial vertex". The set of
oriented edges of G is denoted H, so $|\mathsf{H}| = 2|\mathsf{E}|$. For $h \in \mathsf{H}$, we denote $e(h) \in \mathsf{E}$ the
corresponding unoriented edge and $-h$ the same edge with opposite orientation.
The initial vertex of an oriented edge is denoted $v(h)$, so its terminal vertex is
$v(-h)$.

Remark 3.1. To agree with the language of rotation systems, we call elements of
H half-edges and the adjacency relation is denoted $h \in v$. This terminology is
preferred because vertices correspond to saddle towers and half-edges correspond
to wings of saddle towers.

The number of half-edges adjacent to a vertex v is called the degree of v and
denoted $\deg(v)$. The wings of a saddle tower are naturally ordered by a cyclic
permutation. Accordingly, we define a permutation ς on H as follows: if $h \in v$,
$\varsigma(h) \in v$ is the half-edge which comes after h when traveling around v in the
counterclockwise direction.

3.2. **Formal definition.** In the case that a saddle tower has parallel wings, they
project to the same straight segment in the degenerate limit. Then the intuitive
picture above, which defines edges geometrically, cannot distinguish them properly.
To include this situation, it is necessary to use the language of rotation system.

A *rotation system* consists of a set H and two permutations ι and ς acting on H, such that ι is an involution without fixed points and the group generated by ι and ς acts transitively on H. The elements of H are called half-edges. To ease notations and be consistent with the intuitive picture in Section 3.1, we write $-h$ for $\iota(h)$.

3.2.1. *The multigraph.* The rotation system $(\mathsf{H}, \iota, \varsigma)$ defines a connected multigraph $(\mathsf{H}, \mathsf{V}, \mathsf{E})$, where the vertex set V consists of the orbits of ς and the edge set E consists of the orbits of ι. As we have mentioned before, the vertices correspond to saddle towers, the half-edges correspond to wings, and the edges correspond to glued wing pairs. In this sense, the graph describes the gluing pattern for our construction.

Note that vertices and edges are identified with subsets of H, so $h \in v$ means that the half-edge h is adjacent to the vertex v. For a half-edge $h \in \mathsf{H}$, we use $v(h)$ and $e(h)$ to denote the unique vertex and edge associated to h. We say that $e(h)$ is a *loop* if $v(h) = v(-h)$.

The orbits of $\varsigma\iota$ are called (combinatorial) *faces* of the graph, and the set of faces is denoted by F.

Assumption 3.2. All faces have at least two elements.

Among the edges, we define an equivalence relation known as "parallel", such that $e(h)$ is *parallel* to $e(h')$ whenever $\{h, h'\}$ is a face. Because an equivalence relation is transitive, we have e is parallel to e' whenever there is a sequence $h_0, \cdots, h_n$ such that $e = e(h_0)$, $e' = e(h_n)$, and $\{h_i, h_{i+1}\}$ is a face for all $0 \le i < n$.

3.2.2. *Topological embedding.* The rotation system $(\mathsf{H}, \iota, \varsigma)$ also defines, up to homeomorphism, a 2-cell embedding of the multigraph on a closed oriented surface.

Recall that an embedding represents vertices by distinct points and edges by curves that do not intersect in their interiors. The half-edges then correspond to the curves in small neighborhoods of the vertices. The permutation ς sends a half-edge to the next half-edge around the same vertex in the counterclockwise direction, and ι sends a half-edge to the other half-edge of the same edge.

The connected components of the complement of a 2-cell embedding are all homeomorphic to an open disk, and are called (topological) *faces* of the embedding. They are in correspondence with the combinatorial faces: Half-edges on the boundary of a topological face in the clockwise direction form a combinatorial face of the graph. Note that two edges are parallel if and only if their representatives are homologous.

If the graph is finite, the genus of the oriented surface can be calculated as

$$g = 1 - \frac{1}{2}(|\mathsf{V}| - |\mathsf{E}| + |\mathsf{F}|)$$

and we call this number the *genus* of the graph.

Assumption 3.3. Graphs in the current paper are of genus 1, so they are embedded in a 2-torus $\mathbb{T}^2$.

Remark 3.4. Graphs of genus 0 arise when constructing SPMS instead of TPMS. Higher genus graphs are certainly interesting and could be used to glue saddle towers in $\mathbb{H}^2 \times \mathbb{R}$.

3.2.3. *Geometric representation.* We have seen that the rotation system $(\mathsf{H}, \iota, \varsigma)$ determines a homeomorphism class of 2-cell embeddings. We choose a geometric representation ϱ from the closure of this homeomorphism class. More specifically, ϱ maps vertices to distinct points in a flat torus $\mathbb{T}^2$ and maps each edge to a segment between the images of its endpoints, so that parallel edges are mapped to the same segment, and non-parallel edges are mapped to segments with disjoint interiors.

Such a geometric representation always exists. Indeed, let G' be the graph obtained from G by merging parallel edges. We may apply the genus-one version of Tutte's embedding theorem (see [GGT06] for instance) which implies that G' admits a straight-edge representation on a flat torus. We then obtain a straight-edge representation of G by mapping parallel edges to the same segment that represents the corresponding edge of G'.

3.2.4. *Orientation.* An *orientation* of the graph G is a function $\sigma\colon \mathsf{H} \to \{\pm 1\}$ such that $\sigma(-h) = -\sigma(h)$ for all h.

Definition 3.5. An orientation σ on G is *consistent* if $\sigma \circ \varsigma = -\sigma$. A graph is *orientable* if it admits a consistent orientation. Once a consistent orientation is fixed, we say that the graph is *oriented*.

Note that an orientable graph only has vertices of even degrees. Vertices of degree 2 are not relevant for us, since there is no saddle tower with two wings.

Assumption 3.6. Graphs in this paper have only vertices of degree at least 4.

3.3. **Vector spaces on graphs.**

3.3.1. *Cycles and cuts.* A (simple) *cycle* is a set of half-edges $c \subset \mathsf{H}$ that can be ordered into a sequence $(h_1, \cdots, h_n)$ such that $v(-h_i) = v(h_{i+1})$ for $1 \leq i < n$, $v(-h_n) = v(h_1)$, and $v(h_i) \neq v(h_j)$ whenever $i \neq j$. We use $-c$ to denote the reversed cycle $\{-h\colon h \in c\}$. The set of cycles is denoted by C. In particular, combinatorial faces are all cycles.

For some partition $\mathsf{V} = \mathsf{V}_1 \sqcup \mathsf{V}_2$ of the vertices, the *cut* between V_1 and V_2 is the set of half-edges $b \subset \mathsf{H}$ such that $v(h) \in \mathsf{V}_1$ and $v(-h) \in \mathsf{V}_2$ for all $h \in b$. We use $-b$ to denote the reversed cut $\{-h\colon h \in b\}$. The set of cuts is denoted[1] by B. In particular, for any vertex v, the set

$$b(v) = \{h \in v\colon v(-h) \neq v\}$$

is a cut between $\{v\}$ and $\mathsf{V} \setminus \{v\}$. We call $b(v)$ the *vertex cut* at v.

3.3.2. *Functions on half-edges.* Let $\mathcal{H}$ be the space of functions $f\colon \mathsf{H} \to \mathbb{R}$. We say that $f \in \mathcal{H}$ is *symmetric* if $f_{-h} = f_h$, and *antisymmetric* if $f_{-h} = -f_h$. They can be seen as edge labelings on, respectively, undirected and directed graphs. The orientation σ is an example of antisymmetric function. We use $\mathcal{S}$ and $\mathcal{A}$ to denote, respectively, the space of symmetric and antisymmetric functions.

We denote e_h the characteristic function of $\{h\}$, so $(e_h)_{h \in \mathsf{H}}$ is the canonical basis of $\mathcal{H}$. We equip $\mathcal{H}$ with the inner product $(\cdot, \cdot)$ defined by $(e_h, e_{h'}) = \delta_{h,h'}$. Then $\mathcal{S}$ and $\mathcal{A}$ are orthogonal complementary $|\mathsf{E}|$-dimensional subspaces of $\mathcal{H}$, i.e. $\mathcal{H} = \mathcal{A} \oplus \mathcal{S}$. More specifically, an orthogonal basis for $\mathcal{A}$ is given by

$$a_h = e_h - e_{-h}$$

and an orthogonal basis for $\mathcal{S}$ is given by

$$s_h = e_h + e_{-h}.$$

So any $f \in \mathcal{H}$ can be decomposed into $f = (f^a + f^s)/2$, where $f^a \in \mathcal{A}$ and $f^s \in \mathcal{S}$ are defined by

$$f_h^a = f_h - f_{-h} \quad \text{and} \quad f_h^s = f_h + f_{-h}.$$

---

[1]Inclusion-wise minimal cuts are called *bonds*. Hence the cut space is sometimes referred to as the bond space, therefore our notation.

3.3.3. *Cut space and cycle space.* We use $\mathcal{C}$ to denote the subspace of $\mathcal{A}$ generated by the character functions

$$a_c = \sum_{h \in c} a_h \qquad \text{for } c \in \mathsf{C},$$

known as the *cycle space*. We use $\mathcal{B}$ to denote the subspace of $\mathcal{A}$ generated by the character functions

$$a_b = \sum_{h \in b} a_h \qquad \text{for } b \in \mathsf{B},$$

known as the *cut space*. It is well known [GR01, Chapter 14] that the cut and cycle spaces are orthogonal complementary subspaces of $\mathcal{A}$, i.e. $\mathcal{A} = \mathcal{B} \oplus \mathcal{C}$. The dimension of $\mathcal{C}$ is $|\mathsf{E}| - |\mathsf{V}| + 1$, and the dimension of $\mathcal{B}$ is $|\mathsf{V}| - 1$.

A cut basis is a set $\mathsf{B}^* \subset \mathsf{B}$ such that $(a_b)_{b \in \mathsf{B}^*}$ form a basis of the cut space $\mathcal{B}$. An explicit cut basis is given as follows: Let V^* be the set of all but one vertices. Then $\mathsf{B}^* = \{b(v) : v \in \mathsf{V}^*\}$ is a canonical cut basis. In the following, we write

$$a_v = a_{b(v)} = \sum_{h \in v} a_h,$$

for $v \in \mathsf{V}$.

A cycle basis is a set $\mathsf{C}^* \subset \mathsf{C}$ such that $(a_c)_{c \in \mathsf{C}^*}$ form a basis of the cycle space $\mathcal{C}$. In case G has genus one, the cycle space has dimension $|\mathsf{F}| + 1$ by Euler formula. An explicit cycle basis is given as follows. Let F^* be the set of all but one faces. For $i = 1, 2$, let $c_i \in \mathsf{C}$ be a cycle which is homologous in $\mathbb{T}^2$ to the segment $[0, T_i]$. Then $\mathsf{C}^* = \mathsf{F}^* \cup \{c_1, c_2\}$ is a canonical cycle basis.

3.3.4. *Discrete differential operators.* Let $\mathcal{V}$ be the vector space of functions $f : \mathsf{V} \to \mathbb{R}$ such that $\sum_{v \in \mathsf{V}} f_v = 0$. For $f \in \mathcal{V}$, define

$$\operatorname{grad}(f) = -\sum_{v \in \mathsf{V}} f_v a_v = \sum_{h \in \mathsf{H}} (f_{v(-h)} - f_{v(h)}) e_h.$$

Then $\operatorname{grad} : \mathcal{V} \to \mathcal{B}$ is an isomorphism.

For $f = (f_h)_{h \in \mathsf{H}} \in \mathcal{A}$, define

$$\operatorname{div}_b(f) = (f, a_b)/2 = \sum_{h \in b} f_h, \qquad \operatorname{div}(f) = (\operatorname{div}_b(f))_{b \in \mathsf{B}};$$

$$\operatorname{curl}_c(f) = (f, a_c)/2 = \sum_{h \in c} f_h, \qquad \operatorname{curl}(f) = (\operatorname{curl}_c(f))_{c \in \mathsf{C}}.$$

Because of the orthogonality between $\mathcal{B}$ and $\mathcal{C}$, we have

$$\ker(\operatorname{div}) = \mathcal{C} \quad \text{and} \quad \ker(\operatorname{curl}) = \mathcal{B}.$$

Hence we can identify

$$\operatorname{im}(\operatorname{div}) \simeq \mathcal{B} \quad \text{and} \quad \operatorname{im}(\operatorname{curl}) \simeq \mathcal{C}.$$

Remark 3.7. Let $\pi_\mathsf{B} : \mathbb{R}^{|\mathsf{B}|} \to \mathbb{R}^{|\mathsf{V}|-1}$ be the projection $(x_b)_{b \in \mathsf{B}} \mapsto (x_b)_{b \in \mathsf{B}^*}$. Then $\pi_\mathsf{B} : \operatorname{im}(\operatorname{div}) \to \mathbb{R}^{|\mathsf{V}|-1}$ is an isomorphism. Indeed, $(a_v)_{v \in \mathsf{V}^*}$ is a basis of the cut space so the Gram matrix $(a_v, a_{v'})_{v, v' \in V^*}$ is invertible. In the same way, the projection $\pi_\mathsf{C} : \mathbb{R}^{|\mathsf{C}|} \to \mathbb{R}^{|\mathsf{F}|+1}$, $(x_c)_{c \in \mathsf{C}} \mapsto (x_c)_{c \in \mathsf{C}^*}$ restricts to an isomorphism from $\operatorname{im}(\operatorname{curl})$ to $\mathbb{R}^{|\mathsf{C}|+1}$.

3.4. **A divergence over shortest edges.** For each half-edge h, let ℓ_h° be the length of the segment $\varrho(e(h))$. For $b \in \mathsf{B}$, define

$$\ell_b^\circ = \min_{h \in b} \ell_h^\circ \quad \text{and} \quad m(b) = \{h \in b \mid \ell_h^\circ = \ell_b^\circ\}.$$

We define the operator $\mathrm{mdiv} : \mathcal{A} \to \mathbb{R}^{|\mathsf{B}|}$ by

$$\mathrm{mdiv}_b(\phi) = (a_{m(b)}, \phi)/2 = \sum_{h \in m(b)} \phi_h, \qquad \mathrm{mdiv}(\phi) = (\mathrm{mdiv}_b(\phi))_{b \in \mathsf{B}}.$$

In general, $\mathcal{B}_m := \mathrm{im}(\mathrm{mdiv})$ is different from $\mathcal{B}$, but the following proposition asserts that they have the same dimension.

Proposition 3.8. mdiv *has rank* $|\mathsf{V}| - 1$. *Moreover, there exists a cut basis* B_m^* *such that* $(\mathrm{mdiv}_b)_{b \in \mathsf{B}_m^*}$ *has rank* $|\mathsf{V}| - 1$.

Proof. Let $\phi \in \mathcal{B}$ such that $\mathrm{mdiv}(\phi) = 0$. We can write $\phi = \mathrm{grad}(f)$ with $f \in \mathcal{V}$. Assume that f is not constant. Let V_1 be the set of vertices where f achieves maximum and let b be the corresponding cut. Then $\mathrm{mdiv}(\phi) < 0$, a contradiction. So f is constant and $\phi = 0$. Hence mdiv is injective on $\mathcal{B}$ and

$$\mathrm{rank}(\mathrm{mdiv}) \geq |\mathsf{V}| - 1.$$

For the reverse inequality, consider for $\varepsilon > 0$ the operator $\mathrm{mdiv}^\varepsilon : \mathcal{A} \to \mathbb{R}^{|B|}$ defined by

$$\mathrm{mdiv}_b^\varepsilon(\phi) = \sum_{h \in b} e^{\varepsilon^{-2}(\ell_b^\circ - \ell_h^\circ)} \phi_h, \quad b \in \mathsf{B}.$$

Then

$$\mathrm{mdiv} = \lim_{\varepsilon \to 0} \mathrm{mdiv}^\varepsilon.$$

But we can write for $\varepsilon > 0$

$$\mathrm{mdiv}^\varepsilon = \Phi^\varepsilon \circ \mathrm{div} \circ \Psi^\varepsilon,$$

where

$$\Psi^\varepsilon(\phi) = (e^{-\varepsilon^{-2}\ell_h^\circ} \phi_h)_{h \in \mathsf{H}} \quad \text{and} \quad \Phi^\varepsilon(X) = (e^{\varepsilon^{-2}\ell_b^\circ} X_b)_{b \in \mathsf{B}}.$$

Hence

$$\mathrm{rank}(\mathrm{mdiv}^\varepsilon) \leq \mathrm{rank}(\mathrm{div}) = |\mathsf{V}| - 1.$$

Since the rank is lower semi-continuous, it follows that

$$\mathrm{rank}(\mathrm{mdiv}) \leq |\mathsf{V}| - 1.$$

Hence mdiv has rank $|\mathsf{V}| - 1$. There exists a subset $\mathsf{B}_m^* \subset \mathsf{B}$ with cardinal $|\mathsf{V}| - 1$ such that $(\mathrm{mdiv}_b)_{b \in \mathsf{B}_m^*}$ has rank $|\mathsf{V}| - 1$. Then for $\varepsilon > 0$, $(\mathrm{mdiv}_b^\varepsilon)_{b \in \mathsf{B}_m^*}$ has rank $|\mathsf{V}| - 1$ by continuity, so $(\mathrm{div}_b)_{b \in \mathsf{B}_m^*}$ has rank $|\mathsf{V}| - 1$ and B_m^* is a cut basis. $\qquad\square$

4. Horizontal balance and rigidity

In this part, we assume that $\mathsf{G} = (\mathsf{H}, \iota, \varsigma, \varrho)$ is a finite graph represented in a flat torus $\mathbb{T}^2 = \mathbb{C}/\langle T_1, T_2 \rangle$.

To each half-edge h is associated the unit tangent vector $u_h^\circ = e^{i\theta_h^\circ}$ of the segment $\varrho(e(h))$ at $\varrho(v(h))$. Recall that ℓ_h° denotes the length of the segment $\varrho(e(h))$ and set $x_h^\circ = \ell_h^\circ u_h^\circ$. As a general rule, we use a superscript $\circ$ to denote quantities associated to the given graph G, which are to be perturbed as parameters in the construction.

Remark 4.1. In the intuitive picture in Section 3.1, u_h° is simply the unit vector in the direction of the oriented edge h and ℓ_h° is its length.

Obviously, $u^\circ = (u_h^\circ)_{h \in \mathsf{H}} \in \mathcal{A}^2$, $\ell^\circ = (\ell_h^\circ)_{h \in \mathsf{H}} \in \mathcal{S}$ and $x^\circ = (x_h^\circ)_{h \in \mathsf{H}} \in \mathcal{A}^2$. For $x \in \mathcal{A}^2$ in a neighborhood of x°, we define

$$u_h(x) = \frac{x_h}{\|x_h\|} \quad \text{and} \quad u(x) = (u_h(x))_{h \in \mathsf{H}} \in \mathcal{A}^2.$$

We define the horizontal forces as the function

$$F^{\mathrm{hor}} \colon \mathcal{A}^2 \to \mathcal{B}^2$$

$$x \mapsto \mathrm{div}(u(x)).$$

More explicitly, for any cut $b \in \mathsf{B}$

$$F_b^{\mathrm{hor}}(x) = \sum_{h \in b} \frac{x_h}{\|x_h\|}.$$

Definition 4.2. The graph G is balanced if $F^{\mathrm{hor}}(x^\circ) = 0$.

Remark 4.3. By remark 3.7, the graph is balanced if and only if

$$\sum_{h \in v} \frac{x_h^\circ}{\|x_h^\circ\|} = 0$$

for all $v \in V^*$. In other words, it suffices to consider horizontal forces on a canonical cut basis consisting of all but one vertex cuts.

Remark 4.4. A balanced graph is a weak local minimal network in the sense of Ivanov and Tuzhilin [IT94]; see Proposition B.1 in the Appendix.

Now define the horizontal periods as the operator

$$P^{\mathrm{hor}} \colon \mathcal{A}^2 \to \mathcal{C}^2$$

$$x \mapsto \mathrm{curl}(x).$$

More explicitly, for any cycle $c \in \mathsf{C}$

$$P_c^{\mathrm{hor}}(x) = \sum_{h \in c} x_h.$$

The graph G is represented on the torus $\mathbb{T}^2$ so we have on any canonical cycle basis C^*

$$(1) \qquad P_c^{\mathrm{hor}}(x^\circ) = \begin{cases} 0, & c \in \mathsf{F}^*; \\ T_i, & c = c_i, \quad i = 1, 2. \end{cases}$$

Remark 4.5. The balance and period equations can be compared to Kirchhoff's current and voltage laws of electrical networks. More specifically, u°, x°, and ℓ° play, respectively, the roles of currents, voltages and resistance.

Recall from Section 3.3 that $\ker(P^{\mathrm{hor}}) = \mathcal{B}^2$.

Definition 4.6. The graph G is rigid if the differential $DF^{\mathrm{hor}}(x^\circ)$ restricted to $\ker(P^{\mathrm{hor}})$ is an isomorphism from $\mathcal{B}^2$ to $\mathcal{B}^2$. Equivalently, the graph is rigid if

$$(DF^{\mathrm{hor}}(x^\circ), P^{\mathrm{hor}}) : \mathcal{A}^2 \to \mathcal{A}^2$$

is an isomorphism.

A computation reveals that

$$(2) \qquad DF_b^{\mathrm{hor}}(x^\circ) \cdot \chi = \sum_{h \in b} \frac{1}{\|x_h^\circ\|^3} \left(\langle x_h^\circ, x_h^\circ \rangle \chi_h - \langle x_h^\circ, \chi_h \rangle x_h^\circ \right).$$

The following rigidity result was proved in [You09, Theorem 10].

Theorem 4.7. *Assume that all faces of G have 2 or 3 edges. Then G is rigid.*
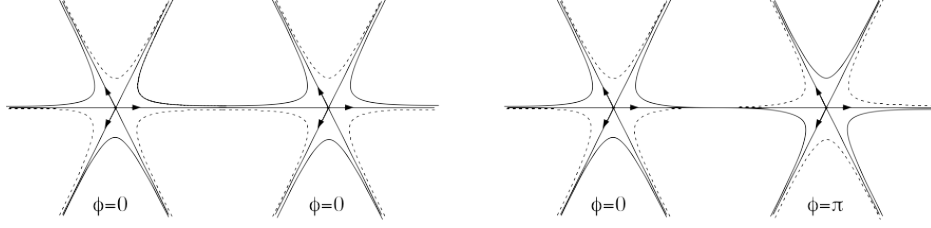
FIGURE 5. Left: two saddle towers in phase. Right: two saddle towers in opposite phase. The solid and dotted lines represent the level lines $x_3 = 0$ and $x_3 = \pi$, respectively.

As [You09] is not published, we include a proof in Appendix B.

Next we need to assign a saddle tower to each vertex.

Definition 4.8. Let $v \in \mathsf{V}$. Consider the convex closed polygon P whose edges are the unit vectors u_h° for $h \in v$ in the order given by the permutation ς. We say that v is *ordinary* if P is neither *degenerate* (appears as a line segment) nor *special* (appears as a parallelogram with two sides of length 1 and two sides of length ≥ 2).

Note that non-ordinary vertices occur only in the presence of parallel edges. If v is ordinary, there exists a saddle tower $\mathscr{S}_v$, unique up to translations, with $\deg(v)$ wings which are in correspondence with the half-edges $h \in v$, so that the direction of the wing corresponding to h is u_h° and the natural order on the wings is given by the permutation ς (see Section 2).

We want to glue the wings of these saddle towers along the edges of G. This construction is achieved if the saddle towers share a horizontal reflection plane, as stated in the following theorem due to Younes [You09].

Theorem 4.9 (TPMSs with horizontal symmetry). *Let G be a graph represented in $\mathbb{T}^2 = \mathbb{C}/\langle T_1, T_2 \rangle$, and assign a phase $\phi_v \in \{0, \pi\}$ to each vertex $v \in \mathsf{V}$. If G is orientable, balanced, rigid, and all vertices are ordinary, then for sufficiently small $\varepsilon > 0$, there is a family $\mathscr{M}_\varepsilon$ of embedded minimal surfaces of genus $|\mathsf{F}| + 1$ in the flat 3-torus*

$$\mathbb{T}_\varepsilon^3 = \mathbb{R}^3/\langle (T_1 \varepsilon^{-2}, 0), (T_2 \varepsilon^{-2}, 0), (0, 0, 2\pi) \rangle.$$

They lift to triply periodic minimal surfaces $\widetilde{\mathscr{M}_\varepsilon}$ in $\mathbb{R}^3$ such that

(1) *$\widetilde{\mathscr{M}_\varepsilon}$ converges, after scaling by ε^2, to $\widetilde{\mathsf{G}} \times \mathbb{R}$ as $\varepsilon \to 0$, where $\widetilde{\mathsf{G}}$ is the lift of G to $\mathbb{R}^2$.*

(2) *For each vertex v of $\widetilde{\mathsf{G}}$, there exists a horizontal vector $X_v(\varepsilon)$ such that $\widetilde{\mathscr{M}_\varepsilon} - X_v(\varepsilon)$ converges on compact subset of $\mathbb{R}^3$ to a saddle tower $\mathscr{S}_v$ as $\varepsilon \to 0$. Moreover, $\varepsilon^2 X_v(\varepsilon) \to \widetilde{\varrho}(v)$ as $\varepsilon \to 0$, where $\widetilde{\varrho}$ is the lift of ϱ.*

(3) *Each limit saddle tower $\mathscr{S}_v$ has phase ϕ_v. Moreover, $\widetilde{\mathscr{M}_\varepsilon}$ is symmetric with respect to a horizontal plane.*

5. CLOSER LOOK ON KARCHER–SCHERK SADDLE TOWERS

We want to break the horizontal symmetry by prescribing phase difference between adjacent saddle towers. The phase differences must satisfy a balancing condition that involves higher order shapes of the Scherk ends. This section is dedicated to a detailed investigation on the saddle towers. Quantities describing the shapes of Scherk ends will be defined in term of Weierstrass representation, and will be useful in the formulation of the main theorem.

5.1. **Weierstrass parameterization of saddle towers.** The quotient of a saddle tower by its vertical period is conformally equivalent to a Riemann sphere $\mathbb{C} \cup \{\infty\}$ with n punctures p_h, $h \in \mathsf{H}$, corresponding to the n wings. The punctures must lie on a circle C fixed by the anti-holomorphic involution ρ corresponding to the horizontal reflections. For convenience, C is often taken to be the unit circle or the real line.

Recall that our saddle tower is scaled so that it has vertical period 2π. Then its Weierstrass data can be written on the punctured Riemann sphere as

$$(3) \qquad \Phi_1 = \sum_{h \in \mathsf{H}} \frac{-\cos\theta_h}{z - p_h} dz, \qquad \Phi_2 = \sum_{h \in \mathsf{H}} \frac{-\sin\theta_h}{z - p_h} dz, \qquad \Phi_3 = \sum_{h \in \mathsf{H}} \frac{-\mathrm{i}\sigma_h}{z - p_h} dz,$$

where the orientation $\sigma_h = \pm 1$ and $\sigma_{\varsigma(h)} = -\sigma_h$ for $h \in \mathsf{H}$. The conformality condition

$$\Phi_1^2 + \Phi_2^2 + \Phi_3^2 = 0$$

determines the punctures p_h up to a Möbius transformation (although doing this explicitly can be difficult). The saddle tower is parameterized by the Weierstrass Representation formula

$$(4) \qquad z \mapsto \operatorname{Re} \int_{z_0}^z \Phi = \operatorname{Re} \int_{z_0}^z (\Phi_1, \Phi_2, \Phi_3).$$

The stereographically projected Gauss map $G = -(\Phi_1 + \mathrm{i}\Phi_2)/\Phi_3$ extends holomorphically to the punctures with $G(p_h) = \mathrm{i}\sigma_h u_h$. Then the Gauss map extends at the end p_h with

$$N(p_h) = \sigma_h(-\sin(\theta_h), \cos(\theta_h), 0).$$

Consequently, the image of the arc between p_h and $p_{\varsigma(h)}$ is a 0-arc if and only if $\sigma_h = 1$.

5.2. **Shape of wings.** Let w_h be a local complex coordinate in a neighborhood of p_h with $w_h(p_h) = 0$. We define

$$\Upsilon_h = \sigma_h \Big\langle N(p_h), \operatorname{Res}\Big(\frac{\Phi}{w_h}, p_h\Big) \Big\rangle_{\mathsf{H}}$$
$$= -\sin(\theta_h) \operatorname{Res}\Big(\frac{\Phi_1}{w_h}, p_h\Big) + \cos(\theta_h) \operatorname{Res}\Big(\frac{\Phi_2}{w_h}, p_h\Big),$$

where $\langle \cdot, \cdot \rangle_{\mathsf{H}}$ denotes the hermitian scalar product on $\mathbb{C}^3$ (semi-linear on the left). Note that Υ_h depends on the local coordinate w_h.

Proposition 5.1.
$$\Upsilon_h = \mathrm{i}\frac{dG}{G \, dw_h}(p_h).$$

Proof. We may expand G and Φ_3 around p_h as

$$G = \mathrm{i}\sigma_h e^{\mathrm{i}\theta_h}\big(1 + aw_h + O(w_h^2)\big),$$
$$G^{-1} = -\mathrm{i}\sigma_h e^{-\mathrm{i}\theta_h}\big(1 - aw_h + O(w_h^2)\big),$$
$$\Phi_3 = -\mathrm{i}\sigma_h\big(\frac{1}{w_h} + b + O(w_h)\big)dw_h,$$

where $a, b \in \mathbb{C}$ and

$$a = \frac{dG}{G \, dw_h}(p_h).$$

This gives

$$\operatorname{Res}\left(\frac{\Phi_1}{w_h}, p_h\right) = -\cos(\theta_h)b - \mathrm{i}\sin(\theta_h)a,$$

$$\operatorname{Res}\left(\frac{\Phi_2}{w_h}, p_h\right) = -\sin(\theta_h)b + \mathrm{i}\cos(\theta_h)a,$$

and

$$\Upsilon_h = -\sin(\theta_h)\left(-\cos(\theta_h)b - \mathrm{i}\sin(\theta_h)a\right) + \cos(\theta_h)\left(-\sin(\theta_h)b + \mathrm{i}\cos(\theta_h)a\right) = \mathrm{i}a.$$

$\square$

We define the quantities

$$\mu_h = \lim_{z \to p_h}\left(e^{\mathrm{i}\theta_h}\log|w_h(z)| + \operatorname{Re}\int_{z_0}^z \Phi_1 + \mathrm{i}\operatorname{Re}\int_{z_0}^z \Phi_2\right),$$

$$\nu_h = \lim_{z \to p_h}\left(-\sigma_h\arg(w_h(z)) + \operatorname{Re}\int_{z_0}^z \Phi_3\right).$$

It is easy to see that the limits exist, but these quantities depend on the local coordinate w_h and the choice of the base point z_0.

Recall that a saddle tower has a horizontal symmetry plane corresponding to an anti-holomorphic involution ρ of the Riemann sphere that fixes all punctures p_h for $h \in \mathsf{H}$.

Definition 5.2. The local coordinate w_h is said to be *adapted* if $w_h \circ \rho = \overline{w_h}$ and $w_h > 0$ near p_h on the arc between p_h and $p_{\varsigma(h)}$.

Proposition 5.3. *Assume that the coordinate w_h is adapted and let ϕ be the phase of the saddle tower. Then $\Upsilon_h > 0$ and*

$$\nu_h = \begin{cases} \phi & \pmod{2\pi} & \text{if } \sigma_h = +1, \\ \phi + \pi & \pmod{2\pi} & \text{if } \sigma_h = -1. \end{cases}$$

Proof. Assume that the coordinate w_h is adapted. We start by computing ν_h. Consider z on the arc between p_h and $p_{\varsigma(h)}$. We have $\arg(w_h) = 0$ for z sufficiently close to p_h. Then, by the definition of the phase ϕ, we have

$$\nu_h = \operatorname{Re}\int_{z_0}^z \Phi_3 = \begin{cases} \phi & \pmod{2\pi} & \text{if } \sigma_h = +1, \\ \phi + \pi & \pmod{2\pi} & \text{if } \sigma_h = -1. \end{cases}$$

Since the coordinate w_h is adapted, we have, for $i = 1, 2$,

$$\rho^*\left(\frac{\Phi_i}{w_h}\right) = \frac{\overline{\Phi_i}}{\overline{w_h}},$$

so $\operatorname{Res}\left(\Phi_i/w_h, p_h\right) \in \mathbb{R}$ and $\Upsilon_h \in \mathbb{R}$.

To understand its sign we need to go back to the Jenkins-Serrin construction. The solution of the Jenkins-Serrin problem is a graph on the convex domain bounded by the polygon P so its Gauss map is non-horizontal in the interior of P. Recalling that the conjugate minimal surface has the same gauss map, we have $|G| \neq 1$ on the Riemann sphere minus the circle C fixed by the symmetry ρ, and $|G| = 1$ on C. Hence in a neighborhood of p_h, $\log G$ is a well-defined holomorphic function and is pure imaginary only on C, so its zero at p_h is simple by the local behavior of holomorphic functions in a neighborhood of a zero. Hence $\Upsilon_h \neq 0$ by Proposition 5.1.

Each horizontal symmetry curve on a saddle tower is a convex curve. Since the unitary vectors u_h are ordered in the counterclockwise order, the argument of G is non-increasing on the arc between p_h and $p_{\varsigma(h)}$. This implies $\Upsilon_h \geq 0$ by Proposition 5.1. $\square$

For a geometric intuition of the quantities Υ_h, μ_h, and ν_h, let us expand the Weierstrass parametrization around p_h:

$$\mathrm{Re}\int_{z_0}^{z}\Phi_1 = \overbrace{\mathrm{Re}\,\mu_h - \cos\theta_h\log|w_h(z)|}^{\text{planar terms}} + \overbrace{\mathrm{Re}\left(w_h(z)\,\mathrm{Res}\left(\frac{\Phi_1}{w_h},p_h\right)\right)}^{\text{undulation terms}} + O(|w_h(z)|^2),$$

$$\mathrm{Re}\int_{z_0}^{z}\Phi_2 = \mathrm{Im}\,\mu_h - \sin\theta_h\log|w_h(z)| + \mathrm{Re}\left(w_h(z)\,\mathrm{Res}\left(\frac{\Phi_2}{w_h},p_h\right)\right) + O(|w_h(z)|^2),$$

$$\mathrm{Re}\int_{z_0}^{z}\Phi_3 = \quad\nu_h \qquad\qquad + \sigma_h\arg(w_h(z)) \qquad\qquad + O(|w_h(z)|).$$

We then observe that

- The terms under the first brace describe a vertical half-plane that passes through (μ_h,ν_h) and extends in the direction θ_h as $w_h(z)\to 0$.
- The terms under the second brace describe a sinusoidal undulation in the vertical coordinate that decays exponentially with the horizontal distance from (μ_h,ν_h); see Figure 3.
- The quantity Υ_h describes the "initial" amplitude of the undulation on the 0-plane in the asymptotic normal direction of the wing.

Remark 5.4. The quantities Υ_h and μ_h behave as follows under change of coordinate: if $\tilde{w}_h$ is another complex coordinate in a neighborhood of p_h and $\tilde{\Upsilon}_h$, $\tilde{\mu}_h$ denote the corresponding quantities, we have, from the definitions,

$$\Upsilon_h = \tilde{\Upsilon}_h\frac{d\tilde{w}_h}{dw_h}(p_h) \quad\text{and}\quad \tilde{\mu}_h - \mu_h = e^{i\theta_h}\log\left|\frac{d\tilde{w}_h}{dw_h}(p_h)\right|.$$

Also observe that $\frac{d\tilde{w}_h}{dw_h}(p_h) > 0$ if both coordinates are adapted.

5.3. **Examples.** In this section, we compute the quantities Υ_h and μ_h for certain saddle towers with explicitly known Weierstrass data. The punctures p_h will be placed on the unit circle in the clockwise order, so we use the adapted coordinate

$$w_h = \mathrm{i}\,\frac{z - p_h}{z + p_h}.$$

With this choice, we have for $h \in \mathsf{H}$

$$(5)\qquad\qquad \mu_h = -e^{\mathrm{i}\theta_h}\log 2 - \sum_{j\neq h}e^{\mathrm{i}\theta_j}\log|p_h - p_j|.$$

5.3.1. *Symmetrically deformed saddle towers.* These examples are described in [Kar88, §2.4.1]. They have $n = 2k$ ends with $k \geq 2$. Their Weierstrass data are given by

$$G = z^{k-1} \quad\text{and}\quad \Phi_3 = \frac{2k\sin(k\varphi)}{z^k + z^{-k} - 2\cos(k\varphi)}\cdot\frac{dz}{z}$$

where $0 < \varphi < \pi/k$. Comparing to [Kar88, §2.4.1], we multiplied Φ_3 by $2k\sin(k\varphi)$ so that the vertical period is 2π.

The punctures are at

$$p_h = \exp\left(-\mathrm{i}\left\lfloor\frac{h}{2}\right\rfloor\frac{2\pi}{k} + \mathrm{i}(-1)^h\varphi\right), \quad 1 \leq h \leq n,$$

we have $\sigma_h = (-1)^h$ and the direction of the wings are

$$\theta_h = \left\lfloor\frac{h}{2}\right\rfloor\frac{2\pi}{k} - (-1)^h\psi, \quad \psi - \frac{\pi}{n} = (k-1)\left(\frac{\pi}{n} - \varphi\right).$$

The case $n = 4$ gives Scherk's surfaces. The case $\psi = \varphi = \pi/n$ gives the most symmetric saddle towers. The saddle towers are embedded for $0 \leq \psi \leq \pi/k$ (with strict inequalities for $n = 4$). If $n \geq 6$, the limit cases $\psi = 0$ and $\psi = \pi/k$ give a

saddle tower with k pairs of parallel wings; an example with $n = 10$ is illustrated on right side of Figure 4.

Given our choice of adapted coordinate and the simple form of the Gauss map, Proposition 5.1 immediately gives

$$\Upsilon_h = n - 2.$$

As for μ_h, Equation (5) does not simplify very much in general, so we only present some special cases. When $n = 4$, (5) simplifies to

$$\mu_h = e^{-i\theta_h} \log \tan(\psi), \quad 1 \le h \le 4,$$

which is not collinear to $e^{i\theta_h}$ unless $\psi = \pi/4$ (see Remark 2.2). For arbitrary n, if $\psi = \pi/n$, then by symmetry, μ_h is collinear to $e^{i\theta_h}$, and its norm (independent of h) is tabulated below for small values of n.

n	$e^{-i\theta_h}\mu_h$
4	0
6	$\log\sqrt{3}$
8	$\sqrt{2}\log(1+\sqrt{2})$
10	$\frac{1}{4}\log 5 + \frac{\sqrt{5}}{2}\log(2+\sqrt{5})$
12	$\frac{1}{2}\log 3 + \sqrt{3}\log(2+\sqrt{3})$

5.3.2. *Isosceles saddle tower with 6 wings.* These examples with $n = 6$ wings are described in [Kar88, §2.5.1]. Their Weierstrass data are given by

$$G = \frac{z^2 + r}{1 + rz^2} \quad \text{and} \quad \Phi_3 = \frac{8\cos(\varphi)^2}{(1-r)^2} \cdot \frac{1 + r^2 + r \cdot (z^2 + z^{-2})}{(z + z^{-1}) \cdot (z^2 + z^{-2} - 2\cos(2\varphi))} \cdot \frac{dz}{z},$$

where $r \in (-1, 1)$ is the unique solution of

$$\frac{4r}{(r-1)^2} = \frac{2\sin(\varphi) - 1}{\cos(\varphi)^2}.$$

Comparing to [Kar88, §2.5.1], we multiplied Φ_3 by $8\cos(\varphi)^2/(1-r)^2$ so that the vertical period is 2π.

The punctures are at

$$(p_0, \cdots, p_5) = (e^{-i\varphi}, -i, -e^{i\varphi}, -e^{-i\varphi}, i, e^{i\varphi}),$$

we have $\sigma_h = (-1)^{h+1}$ and the directions of the wings are

$$(\theta_0, \cdots, \theta_5) = (\psi, \pi/2, \pi - \psi, -\pi + \psi, -\pi/2, -\psi),$$

where $\psi \in (0, \pi/2)$ is the solution of $\sin\psi + \sin\varphi = 1$, so the wings are parallel to the sides of an isosceles triangle. The most symmetric saddle tower is recovered by $\psi = \pi/6$. An example with $\psi = \pi/3$ is illustrated on the left side of Figure 4. The Jenkins–Serrin polygon is degenerate in the limit $\psi \to \pi/2$, and special in the limit $\psi \to 0$.

We compute explicitly

$$r = \frac{\cos(\psi) - \cos(\varphi)}{\cos(\psi) + \cos(\varphi)}$$

$$\Upsilon_h = \begin{cases} 4\cos(\psi)/\cos(\varphi) & h = 1 \pmod 3, \\ 4\cos(\psi)/\sin(2\varphi) & h \ne 1 \pmod 3, \end{cases}$$

$$\mu_0 = i\log\frac{\cos(\varphi)}{1 - \sin(\varphi)} + \exp^{-i\psi}\log\cot(\varphi), \quad \mu_1 = 2i\sin(\psi)\log\frac{\cos(\varphi)}{1 - \sin(\varphi)},$$

and the others μ_h can be obtained by symmetry, namely

$$\mu_0 = -\overline{\mu_2} = -\mu_3 = \overline{\mu_5} \quad \text{and} \quad \mu_1 = -\mu_4.$$

5.4. **Rigidity.** By a result of Cosin-Ros [CR01], all saddle towers are rigid, in the sense that the space of bounded Jacobi fields on a saddle tower is 3-dimensional and consists of translations. This means that when the angles θ_h are fixed, a saddle tower admits no deformation other than translations. In this section, we reformulate this result in term of Weierstrass Representation, in a way that can be used in our gluing construction.

The Weierstrass data of a saddle tower can always be written as in Equation (3). The equation to solve is $Q = 0$, where $Q = \Phi_1^2 + \Phi_2^2 + \Phi_3^2$. Note that Q has at most simples poles at the punctures p_h. The angles θ_h are fixed, and the unknowns are the poles p_h for $h \in \mathsf{H}$. We are given a solution, denoted by p_h°, and we want to study its infinitesimal deformations. The corresponding Weierstrass data is denoted $(\Phi_1^\circ, \Phi_2^\circ, \Phi_3^\circ)$.

We formulate the equation $Q = 0$ as follows. Without loss of generality, we may assume by rotation that $\cos(\theta_h) \neq 0$ for all $h \in \mathsf{H}$ and all zeros of Φ_1° are simple. Then for p in a neighborhood of p°, Φ_1 has $n - 2$ simple zeros $\zeta_1, \cdots, \zeta_{n-2}$ which depend holomorphically on p. The meromorphic 1-form Q/Φ_1 is holomorphic at p_h, $h \in \mathsf{H}$, and has (at most) simple poles at $\zeta_1, \cdots, \zeta_{n-2}$. We define

$$\Lambda(p) = \left(\mathrm{Res}\left(\frac{Q}{\Phi_1}, \zeta_i \right) \right)_{1 \leq i \leq n-3}.$$

By the Residue Theorem, $Q = 0$ is equivalent to $\Lambda(p) = 0$. By a Möbius transformation, we may fix the value of three points p_h, so the parameter p lies in a space of complex dimension $n - 3$.

Theorem 5.5. *The differential $D\Lambda(p^\circ)$ is an isomorphism.*

This theorem is proved in Annexe A of [You09], which is unfortunately not published. So we include a proof in Appendix A.

6. Main result

6.1. **Vertical balance and rigidity.** We prescribe the phase differences between adjacent saddle towers through an antisymmetric *phase function* $\phi^\circ \colon \mathsf{H} \to \mathbb{R}/2\pi\mathbb{Z}$ that assigns a phase difference ϕ_h° to each half-edge h. We say that ϕ° is trivial if $\phi^\circ = 0$ or $\phi^\circ = \pi$ on every half-edge, which is the case in Theorem 4.9.

Define the vertical periods as the function

$$P^{\mathrm{ver}} \colon \mathcal{A} \to \mathcal{C}$$

$$\phi \mapsto \mathrm{curl}(\phi).$$

We require that the periods of the phase function are given on a canonical cycle basis C^* as

$$(6) \qquad P_c^{\mathrm{ver}}(\phi^\circ) = \sum_{h \in c} \phi_h^\circ = \begin{cases} 0, & c \in \mathsf{F}; \\ \Psi_i, & c = c_i, \quad i = 1, 2. \end{cases}$$

for some $\Psi_1, \Psi_2 \in \mathbb{R}/2\pi\mathbb{Z}$. We call Ψ_1 and Ψ_2 the *fundamental shifts*. We want to construct minimal surfaces in the flat 3-torus

$$\mathbb{T}_\varepsilon^3 = \mathbb{R}^3 / \langle (\Lambda_1 + T_1 \varepsilon^{-2}, \Psi_1), (\Lambda_2 + T_2 \varepsilon^{-2}, \Psi_2), (0, 0, 2\pi) \rangle,$$

Here Λ_1, Λ_2 are fixed complex numbers that prescribe a first order horizontal deformation of the lattice as ε varies.

The phase function must satisfy a balancing condition, which we now explain.

For each vertex $v \in \mathsf{V}$, let $\hat{\mathbb{C}}_v$ be the punctured Riemann sphere on which the saddle tower $\mathscr{S}_v$ is parametrized. Fix an adapted local coordinate w_h in a neighborhood of the puncture $p_h \in \mathbb{C}_{v(h)}$ for every $h \in \mathsf{H}$. Recall the definition of

the numbers Υ_h, μ_h in Section 5 and the notation $\mu_h^a = \mu_h - \mu_{-h}$. If the graph G is balanced and rigid, the system

$$(7) \quad \begin{cases} DF_b^{\mathrm{hor}}(x^\circ) \cdot \xi = 0, & b \in \mathsf{B}; \\ P_c^{\mathrm{hor}}(\xi) = -P_c^{\mathrm{hor}}(\mu^a), & c \in \mathsf{F}^*; \\ P_{c_i}^{\mathrm{hor}}(\xi) = -P_{c_i}^{\mathrm{hor}}(\mu^a) + \Lambda_i, & i = 1, 2 \end{cases}$$

has a unique solution $\xi \in \mathcal{A}^2$ by Definition 4.6 and Remark 3.7.

Remark 6.1. The system (7) is invariant by horizontal translations of the saddle towers. Indeed, if $\mathscr{S}_v$ is translated by a horizontal vector X_v, then $X_{v(h)}$ is added to μ_h, so $\mathrm{curl}(\mathrm{grad}(X)) = 0$ is added to the right-hand side of (7).

We define a symmetric function

$$(8) \quad K_h = \Upsilon_h \Upsilon_{-h} e^{-\mathrm{Re}(\xi_h \overline{u_h^\circ})}.$$

By Proposition 5.3, we have $K_h > 0$. We will see in Proposition 6.10 that K_h is independent of the choice of adapted coordinates w_h. Both ξ and K_h depend on Λ_1 and Λ_2, but the dependence is omitted for simplicity. When the values of Λ_1 and Λ_2 matter, but are not specified in the context, it is implied that $\Lambda_1 = \Lambda_2 = 0$.

We define the vertical forces as the function

$$F^{\mathrm{ver}} \colon \mathcal{A} \to \mathcal{B}_m$$

$$\phi \mapsto \mathrm{mdiv}\left((K_h \sin \phi_h)_{h \in \mathsf{H}}\right).$$

More explicitly, for any cut $b \in \mathsf{B}$

$$F_b^{\mathrm{ver}}(x) = \sum_{h \in m(b)} K_h \sin(\phi_h).$$

Definition 6.2. The phase function ϕ° is balanced if $F^{\mathrm{ver}}(\phi^\circ) = 0$.

Remark 6.3. Trivial phase functions are trivially balanced.

Remark 6.4. Unlike horizontal balancing (see Remark 4.3), the equation $F^{\mathrm{ver}}(\phi^\circ) = 0$ is in general not equivalent to $F_{b(v)}^{\mathrm{ver}}(\phi^\circ) = 0$ for $v \in \mathsf{V}^*$: it is not enough to consider vertex cuts; see Example 7.6. This is the reason why it is necessary to introduce the whole cut space to define vertical balancing.

Remark 6.5. In general, the vertical forces do not depend continuously on the horizontal periods T_1 and T_2, but they depend continuously on the deformations Λ_1 and Λ_2.

Definition 6.6. The phase function ϕ° is rigid if the differential $DF^{\mathrm{ver}}(\phi^\circ)$ restricted to $\mathcal{B}$ is an isomorphism between $\mathcal{B}$ and $\mathcal{B}_m$. Equivalently, the phase function is rigid if $(DF^{\mathrm{ver}}(\phi^\circ), P^{\mathrm{ver}})$ is an isomorphism.

We call the pair (G, ϕ°) a *configuration*. We say that the configuration is horizontally balanced (resp. rigid) if the graph is balanced (resp. rigid), and vertically balanced (resp. rigid) if the phase function is balanced (resp. rigid). And we say that the configuration is balanced (resp. rigid) if it is both horizontally and vertically balanced (resp. rigid). Our main result for TPMSs is the following.

Theorem 6.7 (TPMSs). *Let (G, ϕ°) be a configuration, where the graph G is represented in $\mathbb{T}^2 = \mathbb{C}/\langle T_1, T_2 \rangle$, and the fundamental shifts of ϕ° is Ψ_1 and Ψ_2. Assume that G is orientable, that the configuration is balanced and rigid, and that all vertices are ordinary. Then for sufficiently small $\varepsilon > 0$, there is a family $\mathscr{M}_\varepsilon$ of embedded minimal surfaces of genus $|\mathsf{F}| + 1$ in the flat 3-torus*

$$\mathbb{T}_\varepsilon^3 = \mathbb{R}^3 / \langle (\Lambda_1 + T_1 \varepsilon^{-2}, \Psi_1), (\Lambda_2 + T_2 \varepsilon^{-2}, \Psi_2), (0, 0, 2\pi) \rangle.$$

They lift to triply periodic minimal surfaces $\widetilde{\mathscr{M}_\varepsilon}$ in $\mathbb{R}^3$ such that

(1) $\widetilde{\mathscr{M}}_\varepsilon$ *converges, after a scaling by* ε^2*, to* $\widetilde{\mathsf{G}} \times \mathbb{R}$ *as* $\varepsilon \to 0$*, where* $\widetilde{\mathsf{G}}$ *is the lift of* G *to* $\mathbb{R}^2$*.*

(2) *For each vertex* v *of* $\widetilde{\mathsf{G}}$*, there exists a horizontal vector* $X_v(\varepsilon)$ *such that* $\widetilde{\mathscr{M}}_\varepsilon - X_v(\varepsilon)$ *converges on compact subset of* $\mathbb{R}^3$ *to a saddle tower* $\mathscr{S}_v$ *as* $\varepsilon \to 0$*. Moreover,* $\varepsilon^2 X_v(\varepsilon) \to \widetilde{\varrho}(v)$ *as* $\varepsilon \to 0$*, where* $\widetilde{\varrho}$ *is the lift of* ϱ*.*

(3) *For each half-edge* h*, the phase difference of* $\mathscr{S}_{v(-h)}$ *over* $\mathscr{S}_{v(h)}$ *is equal to* ϕ_h°*.*

Remark 6.8. Unfortunately, Theorem 6.7 does not contain Theorem 4.9 as a particular case. A trivial phase function is trivially balanced, but it is not necessarily rigid. However, Proposition 6.12 below implies that the phase function is rigid when ϕ_h°, $h \in \mathsf{H}$, are all 0 or all π. So Theorem 4.9 follows from Theorem 6.7 when all saddle towers are in-phase, or all adjacent saddle towers are anti-phase.

Remark 6.9. In fact, we construct a continuous family locally parameterized by ε, $\Lambda_{1,2}$, and $\Psi_{1,2}$. By Proposition 6.11 below, we may assume that $\Lambda_1 = 0$ up to a scaling and a horizontal rotation. This is therefore a 5-parameter family up to Euclidean rotations and scalings, in correspondence with the deformations of the lattice.

6.2. **Some auxiliary results.**

Proposition 6.10. *The constant* K_h *defined in Equation* (8) *is independent of the adapted local coordinates* w_h*.*

Proof. Consider another adapted local coordinates $\tilde{w}_h$ in a neighborhood of p_h for each $h \in \mathsf{H}$. We use a tilde for all quantities associated to the coordinate $\tilde{w}_h$. By Remark 5.4, we have, writing $\kappa_h = \frac{d\tilde{w}_h}{dw_h}(p_h) > 0$, that

$$\tilde{\mu}_h - \mu_h = u_h^\circ \log \kappa_h \quad \text{and} \quad \tilde{\Upsilon}_h = \Upsilon_h / \kappa_h.$$

Therefore, since $u_{-h}^\circ = -u_h^\circ$

$$\tilde{\mu}_h^a - \mu_h^a = u_h^\circ \log(\kappa_h \kappa_{-h}).$$

Observe that $\tilde{\xi} - \xi$ is the solution of

$$\begin{cases} DF^{\text{hor}}(x^\circ) \cdot (\tilde{\xi} - \xi) = 0; \\ P^{\text{hor}}(\tilde{\xi} - \xi) = -P^{\text{hor}}(\tilde{\mu}^a - \mu^a). \end{cases}$$

By Equation (2), we have

$$DF^{\text{hor}}(x^\circ) \cdot (\tilde{\mu}_h^a - \mu_h^a) = 0.$$

So the solution is trivially

$$\tilde{\xi}_h - \xi_h = -\tilde{\mu}_h^a + \mu_h^a = -u_h^\circ \log(\kappa_h \kappa_{-h}), \quad h \in \mathsf{H}.$$

Therefore,

$$\frac{\tilde{K}_h}{K_h} = \frac{\tilde{\Upsilon}_h}{\Upsilon_h} \frac{\tilde{\Upsilon}_{-h}}{\Upsilon_{-h}} \exp\left(-\operatorname{Re}\left((\tilde{\xi}_h - \xi_h)\overline{u_h^\circ}\right)\right) = \frac{e^{\log(\kappa_h \kappa_{-h})}}{\kappa_h \kappa_{-h}} = 1.$$

$\square$

Proposition 6.11. *The vertical balance condition is invariant under the transform* $\Lambda_i \mapsto \tilde{\Lambda}_i = \Lambda_i + \lambda T_i$, $\lambda \in \mathbb{C}$*.*

Proof. We use a tilde for all quantities associated to $\tilde{\Lambda}_i$. Using Equations (1) and (2), the solutions of (7) satisfy $\tilde{\xi} - \xi = \lambda x^\circ$. Hence $\tilde{K}_h = K_h \exp(-\ell_h^\circ \operatorname{Re} \lambda)$ and $\tilde{F}_b^{\text{ver}} = F_b^{\text{ver}} \exp(-\ell_b^\circ \operatorname{Re} \lambda)$. $\square$

We conclude this section with the following vertical rigidity result:

Proposition 6.12. *Let ϕ° be a phase function such that $\cos(\phi_h^\circ)$, $h \in \mathsf{H}$, are all positive or all negative. Then ϕ° is rigid. In particular, the zero phase function is always balanced and rigid.*

Proof. It suffices to prove the case where $\cos(\phi_h^\circ)$ are all positive. Let $\dot\phi \in \mathcal{B}$ such that $DF_b^{\mathrm{ver}}(\phi^\circ) \cdot \dot\phi = 0$. We can write $\dot\phi = \mathrm{grad}(f)$ with $f \in \mathcal{V}$. Then

$$0 = dF_b^{\mathrm{ver}}(\phi^\circ) \cdot \dot\phi = \sum_{h \in m(b)} K_h \cos(\phi_h^\circ)(f_{v(-h)} - f_{v(h)}).$$

Since $K_h \cos(\phi_h^\circ) > 0$ for all $h \in \mathsf{H}$, we conclude that $\dot\phi = 0$ by the same argument as in the proof of Proposition 3.8, considering the maximum of f. $\qquad\square$

7. Examples

In this part, examples are sketched in the form of diagrams. Edges are decorated with arrows to illustrate a consistent orientation σ. Unless otherwise specified (e.g. Example 7.7), for each h such that $\sigma(h) = 1$, we label the phase difference ϕ_h° on the edge $e(h)$. The fundamental parallelogram of the torus spanned by T_1 and T_2 is illustrated by dotted lines.

For all the examples presented below, the computation of K_h is either trivial because of symmetry, or not necessary (e.g. Examples 7.2).

7.1. **Genus three.** The genus of a TPMS is at least three, hence the graph for our construction has at least two faces. We notice four families of balanced configurations with two faces. They are illustrated in Figure 6. Theorem C.1 in the Appendix asserts that these are the only balanced configurations whose graphs are orientable with two faces. Hence they are the only possible configurations that give rise to TPMSs of genus 3.
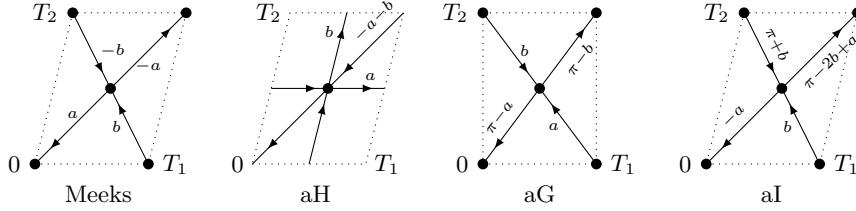

FIGURE 6. The four balanced configurations that could give rise to TPMSs of genus three.

Example 7.1 (Meeks family)**.** The first diagram illustrates a 4-parameter family (parameterized by T_1, T_2, a, and b). It actually describes the Scherk limit of Meeks' family [Mee90]. To see this, note that the configurations are invariant under the translation $(T_1 + T_2)/2$. This implies an orientation-reversing translational symmetry in the corresponding TPMSs, which characterizes Meeks' surfaces. See Figures 2(a–c) for examples in this family.

Let us work out this small example explicitly. The graph is clearly balanced and rigid. Let v be the center vertex, and label 1, 2, 3, 4 the half-edges adjacent to v in anti-clockwise order, starting with the half-edge marked a. Then the horizontal period condition (1) on any face cycle gives

$$\phi_1 - \phi_2 + \phi_3 - \phi_4 = 0$$

and the fundamental shifts are given by

$$\Psi_1 = -\phi_1 + \phi_2 \quad \text{and} \quad \Psi_2 = -\phi_1 + \phi_4.$$

- If T_1 and T_2 are orthogonal, all edges have the same length so $m(b(v)) = \{1, 2, 3, 4\}$ and

$$F_{b(v)}^{\mathrm{ver}}(\phi) = K \left(\sin(\phi_1) + \sin(\phi_2) + \sin(\phi_3) + \sin(\phi_4) \right).$$

  A solution is $(\phi_1, \phi_2, \phi_3, \phi_4) = (a, -b, -a, b)$ with $a = \frac{-\Psi_1 - \Psi_2}{2}$ and $b = \frac{\Psi_2 - \Psi_1}{2}$. Regarding rigidity, we have $\dot{\phi} \in \ker(P^{\mathrm{ver}}, DF^{\mathrm{ver}}(\phi))$ if and only if

$$\begin{cases} \dot{\phi}_1 - \dot{\phi}_2 + \dot{\phi}_3 - \dot{\phi}_4 = 0 \\ -\dot{\phi}_1 + \dot{\phi}_2 = 0 \\ -\dot{\phi}_1 + \dot{\phi}_4 = 0 \\ \cos(a)(\dot{\phi}_1 + \dot{\phi}_3) + \cos(b)(\dot{\phi}_2 + \dot{\phi}_4) = 0 \end{cases}$$

  which gives $\dot{\phi} = 0$ if $\cos(a) + \cos(b) \neq 0$, so the configuration is vertically rigid if $\cos(a) + \cos(b) \neq 0$.
- If $\arg(T_2/T_1) < \pi/2$, the edges $e(2)$ and $e(4)$ are shorter so $m(b(v)) = \{2, 4\}$ and

$$F_{b(v)}^{\mathrm{ver}}(\phi) = K \left(\sin(\phi_2) + \sin(\phi_4) \right).$$

  The solution $(a, -b, -a, b)$ is rigid if $\cos(b) \neq 0$.
- If $\arg(T_2/T_1) > \pi/2$, the edges $e(1)$ and $e(3)$ are shorter, so $m(b(v)) = \{1, 3\}$ and the solution $(a, -b, -a, b)$ is rigid if $\cos(a) \neq 0$. $\qquad \square$

Example 7.2 (aH)**.** The second diagram is again a 4-parameter family. We name it aH because, when $|T_1| = |T_2|$ and $a = b = 0$, it gives Scherk limits of the oH family [CW21]; see Figure 2(d). Another special case in this family is the Scherk limit of the rhombohedral deformation family rGL of the Gyroid [Che21], given by $T_2/T_1 = \exp(2i\pi/3)$ and $a = b = 2\pi/3$; see Figure 1 (left). All configurations in the family are rigid, hence give rise to a new 5-parameter family of TPMSs, generalizing H and rGL. $\qquad \square$

Previously, we knew that both the Gyroid and the H surfaces can be continuously deformed to Meeks surfaces [Che21, CW21]. The aH family implies a deformation path between them that does not pass through the Meeks family.

Corollary 7.3. *The Gyroid can be continuously deformed to an H surface along a path in the space of TPMSs of genus 3 that stays outside the Meeks family.*

Example 7.4 (aG)**.** The third diagram is constrained to $\arg(T_2/T_1) = \pi/2$, hence a 3-parameter family. One of the fundamental shift must be π. We name it aG as it includes the Scherk limit of the tetragonal deformation family tG of the Gyroid [Che21], given by $|T_1| = |T_2|$ and $a = b = \pi/2$; see Figure 1 (right). It intersects Meeks family when $a = b = 0$. Moreover, when $a = 0$ and $b = \pi$, we recognize alternative Scherk limits of the oH family [CW21]; see Figure 2(e).

Unfortunately, configurations in this family are not vertically rigid, hence our construction is inconclusive for them. To see this, note that adding a common constant to a and b does not change the fundamental shifts. For the corresponding TPMSs, this seems to suggest that one can vertically slide one Scherk tower with respect to the other without changing the lattice. Numerical experiments suggest that these configurations give indeed rise to TPMSs, but a vertical sliding between the towers must be accompanied by a very slight deformation of the horizontal lattice, which becomes undetectable in the Scherk limit. $\qquad \square$

Example 7.5 (aI)**.** The fourth diagram is again a 4-parameter family, but constrained to $\arg(T_2/T_1) \neq \pi/2$. The fundamental shifts satisfy $\Psi_2 - \Psi_1 = \pi$. When $\Psi_1 = \pi$, it tends to aG configurations as $\arg(T_2/T_1) \to \pi/2$. Otherwise, the dependence of the vertical balancing condition on the horizontal lattice is not continuous; see Remark 6.5.

Configurations in this family are not vertically rigid: adding a common constant to a and b does not change the fundamental shifts. Our construction is inconclusive and, apart from the aG limit, we are not aware of any known TPMS that admits this kind of Scherk limit. But by Theorem 4.9, the trivial phase functions given by $a, b = 0$ or π should give rise to a family of TPMSs. For a lack of a better name, we call this family aI (following the pattern of aG, aH.) $\square$

7.2. Technical examples with triangular lattice.

Example 7.6. The purpose of this example is to demonstrate the necessity to define vertical balancing on the whole cut space.

Figure 7 illustrates a graph with four vertices. If only vertex cuts are considered, solving the vertical balancing equation would only determine phase differences on the four vertical edges. This gives a false illusion that one may vertically slide the saddle towers with respect to each other. In fact, to determine phase differences on the remaining edges, we must acknowledge that they form a cut and must also be balanced. $\square$
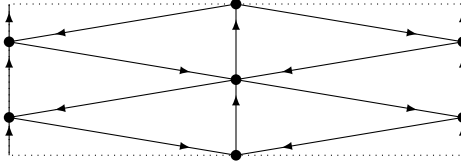

FIGURE 7. For vertical balancing on this graph, it is not enough to consider only vertex cuts.

Example 7.7. The purpose of this example is to demonstrate the diversity of balanced phase functions.

The graph in Figure 8, which is a 3×3 block of the triangular lattice, is trivially balanced and rigid by Theorem 4.7. Unlike other diagrams in this section, the phases of the saddle towers are labeled on the vertices up to the addition of a common constant. This is possible because the fundamental shifts are 0.

On this small graph, we look for phase functions symmetric in the points marked with empty circles in the figure. That is,

$$\phi_1 = -\phi_2, \quad \phi_3 = -\phi_6, \quad \phi_4 = -\phi_8, \quad \phi_5 = -\phi_7.$$

Under these strict restrictions, we still find two non-trivial, balanced, and rigid phase functions, namely

- $-\phi_1 = \phi_2 = 2\pi/3$, $-\phi_3 = \phi_5 = \phi_6 = -\phi_7 = \pi/3$, and $\phi_4 = -\phi_8 = \pi$;
- $\phi_1 = -\phi_2 = -\phi_3 = \phi_5 = \phi_6 = -\phi_7 = 2\arctan\sqrt{5/7}$ and $\phi_4 = -\phi_8 = \pi$.

For readers who are interested in double checking: the rigidities are confirmed numerically by computing the determinant of an 8×8 Jacobian matrix, which is the derivative of vertical forces on 8 vertices with respect to their phases. If we assume $K_h = 1$ on all half-edges (up to scaling of local coordinates), the Jacobian determinant is $-3/4$ for the first phase function, and $-315/4$ for the second.

We certainly did not find all non-trivial, balanced, and rigid phase functions on this graph. It can be imagined that, if we take a larger block of triangular lattice or relax the inversion symmetry, there will be more balanced and rigid phase functions. $\square$
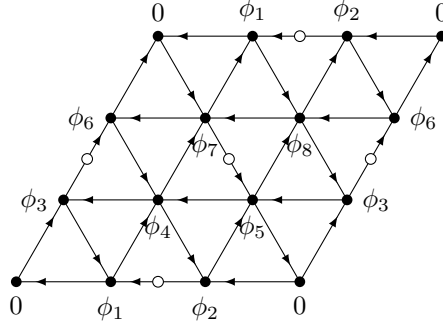
FIGURE 8. A configuration with the graph of the triangular lattice. Phase functions are labeled on the vertices instead of the edges. We look for phase functions symmetric in the points marked with the empty circles.

7.3. **Generalizing some known examples.** We generalize here some interesting known examples to demonstrate the power of our construction. Many known families of TPMSs admit saddle tower limits. In addition to those discussed below, examples also include Schoen's so-called RII, RIII, I-6, I-8, I-9[2], and GW surfaces [Sch70, Bra], and many more constructed in [FK87, Kar89]. Brakke's webpage [Bra] is a great source of examples. We certainly do not plan to discuss all of them.

If a graph contains a pair of parallel edges, they must be adjacent, and their orientations and phase differences must all be opposite. In fact, given any graph $\mathsf{G} = (\mathsf{H}, \iota, \varsigma, \varrho)$ with only simple edges, we may construct a *doubling graph* $\bar{\mathsf{G}} = (\bar{\mathsf{H}}, \bar{\iota}, \bar{\varsigma}, \bar{\varrho})$ with only parallel edges as follows (we use a bar for all objects associated to $\bar{\mathsf{G}}$).

- For each $h \in \mathsf{H}$, we have two half-edges $\bar{h}_+, \bar{h}_- \in \bar{\mathsf{H}}$;
- We define $\bar{\iota}$ by $\bar{\iota}(h_+) = (\iota(h))_-$ and $\bar{\iota}(h_-) = (\iota(h))_+$;
- We define $\bar{\varsigma}$ by $\bar{\varsigma}(h_+) = h_-$ and $\bar{\varsigma}(h_-) = (\varsigma(h))_+$;
- We define $\bar{\varrho}$ by $\bar{\varrho}(\bar{v}(\bar{h}_\pm)) = \varrho(v(h))$ and $\bar{\varrho}(\bar{e}(\bar{h}_\pm)) = \varrho(e(h))$.

Clearly, the doubling graph $\bar{\mathsf{G}}$ is always orientable, even if the original graph G is not. This observation expands the power of our constructions: Even if the graph is not orientable, as long as a graph is balanced and rigid, its doubling would be an orientable, balanced, and rigid graph.
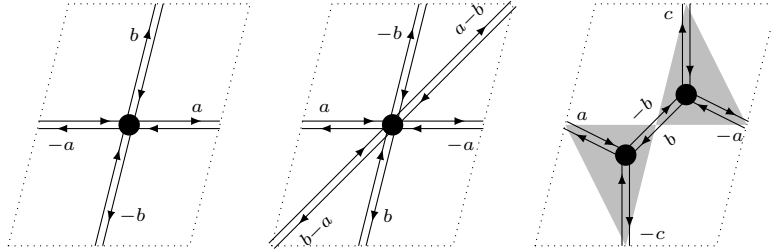

FIGURE 9. Configurations doubling the graphs of parallelogram, triangle and hexagonal tilings.

---

[2]These names are coined by Brakke for they are the 6th, 8th, and 9th surface on Page I of a note by Schoen.

Example 7.8. In Figure 9, we illustrate three configurations that double the graphs of tilings of the Euclidean plane. Each diagram describes a 4-parameter family of balanced configurations. They generalize, respectively, the Scherk limits of Schoen's S'–S", T'–R', and H"–R families [Sch70]; see Figures 2(g–i). The first two configurations in the figure are trivially balanced and rigid, hence give rise to 5-parameter families of TPMSs.

As for the last one that doubles hexagonal tilings, the graph is balanced if and only if the vertices are at the unique Fermat–Torricelli points of the gray triangles spanned by the 2-division points of the torus. This is well defined only when these triangles do not have an angle $\geq 2\pi/3$. Let l_a, l_b and l_c be the lengths of the edges labeled by $\pm a$, $\pm b$ and $\pm c$ in the figure, respectively. We may assume that $l_a \leq l_b \leq l_c$. Then the balance condition for the phase function is

$$\left.\begin{array}{r} e^{\mathrm{i}a} \\ e^{\mathrm{i}a} + e^{\mathrm{i}b} \\ e^{\mathrm{i}a} + e^{\mathrm{i}b} + e^{\mathrm{i}c} \end{array}\right\} \text{ being real, if } \left\{\begin{array}{l} l_a < l_b \leq l_c; \\ l_a = l_b < l_c; \\ l_a = l_b = l_c. \end{array}\right.$$

The phase function is rigid if the left hand side is non-zero.

We see again that balancing conditions do not depend continuously on the horizontal lattice. But the dependence on Λ_1 and Λ_2 is continuous, so the rigid configurations still give rise to 5-parameter families of TPMSs. See Remark 6.5. $\qquad\square$

We end the section with the saddle tower limit of a known TPMS family, which is however not horizontally rigid.

Example 7.9. On the left of Figure 10 is a configuration that generalizes the Scherk limit of Schoen's H'–T family [Sch70] (with $T_2/T_1 = \exp(\mathrm{i}\pi/3)$ and $a = b = 0$; see Figure 2(f)). The graph is obviously balanced but, unfortunately, not rigid. To see this, notice that the graph is represented as the union of three lines. Any of the lines can be moved parallelly yet the graph remains balanced. As a consequence, our construction does not work directly on this graph.

But we may impose an inversion symmetry in the vertices. Under this imposed symmetry, the phase function must have the form as shown in the figure. The configurations form a 4-parameter family. They are trivially balanced and rigid modulo symmetries. Our construction works with little modification, and gives rise to a 5-parameter family of TPMSs of genus 4 generalizing the H'–T surfaces. We do not plan to write down the details. $\qquad\square$
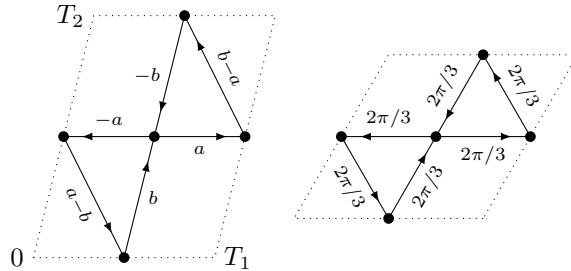

FIGURE 10. Left: Configurations generalizing the Scherk limit of Schoen's H'–T family. Right: Scherk limit of the QTZ–QZD family, a chiral generalization of H'–T.

Remark 7.10. Recently, a chiral variation of H'–T was discovered and named QTZ–QZD [MSSTM18]. It arises from the same graph as H'–T, but has a non-trivial phase function; see the right side of Figure 10.

8. Construction

In this section, we prove Theorem 6.7. The given phase function is denoted ϕ°. All parameters will vary in a neighborhood of a central value denoted with a superscript $\circ$, which depends on the given configuration (G, ϕ°). The Implicit Function Theorem will be applied at $\varepsilon = 0$ and the central value of all parameters.

Without loss of generality, we assume as in Section 5.4 that $\cos(\theta_h^\circ) \neq 0$ for all $h \in \mathsf{H}$ and that the zeros of Φ_1 are simple for all saddle towers involved in the construction. If this is not the case, we could always apply a horizontal rotation to the configuration.

8.1. Opening nodes.
For each vertex $v \in \mathsf{V}$, we want to place a saddle tower $\mathscr{S}_v$ determined by the angles θ_h°, $h \in v$, and glue them along the wings.

Recall that a saddle tower is conformally a sphere with punctures corresponding to the wings. Hence our initial surface at $\varepsilon = 0$ is a singular Riemann surface consisting of $|\mathsf{V}|$ spheres identified at their punctures. More specifically: to each vertex $v \in \mathsf{V}$ of the oriented graph G, we associate a Riemann sphere $\hat{\mathbb{C}}_v$. To each half-edge $h \in v$, we associate a complex number $p_h^\circ \in \hat{\mathbb{C}}_v$, so that $\hat{\mathbb{C}}_v$ punctured at p_h°, $h \in v$, provides a conformal model for $\mathscr{S}_v$. Then we identify p_h° and p_{-h}°. The resulting singular Riemann surface with nodes is denoted Σ_0.

As ε increases, we want to desingularize the nodes into necks. This is done as follows. For each $h \in \mathsf{H}$, p_h is a complex parameter in a neighborhood of p_h°. Consider a local coordinate w_h in a neighborhood of $p_h \in \hat{\mathbb{C}}_{v(h)}$ such that $w_h(p_h) = 0$. The local coordinate w_h depends holomorphically on p_h, but the dependence is omitted for simplicity. Moreover, we assume that the local coordinate w_h° associated to p_h° is adapted. We denote $p = (p_h)_{h \in \mathsf{H}}$.

Since the graph is finite, it is possible to fix a small number $\delta > 0$ independent of v such that the disks $|w_h^\circ| < 2\delta$ for $h \in v$ are disjoint in each Riemann sphere $\hat{\mathbb{C}}_v$. Then for p close enough to p°, the disks $|w_h| < \delta$ for $h \in v$ are disjoint.

Consider a symmetric complex parameter $t = (t_h)_{h \in \mathsf{H}}$ in the neighborhood of 0 with $|t_h| < \delta^2$. For every $h \in \mathsf{H}$, if $t_h \neq 0$, we remove the disk

$$|w_h| < |t_h|/\delta,$$

and identify the annuli

$$|t_h|/\delta \leq |w_h| \leq \delta \quad \text{and} \quad |t_{-h}|/\delta \leq |w_{-h}| \leq \delta$$

by

$$w_h w_{-h} = t_h.$$

When $t_h = 0$, p_h and p_{-h} are simply identified to form a node. This produces a Riemann surface, possibly with nodes, denoted by Σ_t. Note that Σ_t also depends on the parameter p, but the dependence is not written for simplicity. When $t_h \neq 0$ for all $h \in \mathsf{H}$, Σ_t is a regular Riemann surface of genus $g = |\mathsf{F}| + 1$ which provides the conformal model for our construction.

We consider the following fixed domains in all Σ_t:

$$U_{v,\delta} = \{z \in \hat{\mathbb{C}}_v : \forall h \in v, \ |w_h^\circ| > \delta/2\} \quad \text{and} \quad U_\delta = \bigsqcup_{v \in \mathsf{V}} U_{v,\delta}$$

For $v \in \mathsf{V}$, we denote ∞_v the point at infinity in the Riemann sphere $\hat{\mathbb{C}}_v$ and fix an origin $O_v \in U_{v,\delta} \setminus \{\infty_v\}$ as the starting point of the integration defining the Weierstrass parameterization of the saddle tower $\mathscr{S}_v$.

8.2. **Regular 1-forms.** Let Σ_t be a family of Riemann surfaces defined by opening nodes as above. A *regular 1-form* ω on Σ_t is a differential 1-form that is holomorphic away from the nodes and, whenever two points p and q are identified to form a node, has simple poles of opposite residues at p and q. Regular 1-forms extend the notion of holomorphic 1-forms to noded Riemann surfaces. By [Mas76, Proposition 4.1], there is a basis $\omega_{1,t}, \cdots, \omega_{g,t}$ for the space of regular 1-forms on Σ_t which "depends holomorphically" on t in a neighborhood of 0. More formally, in our case, this means that the restriction of $\omega_{j,t}$ to U_δ depends holomorphically on $z \in U_\delta$ and t.

One can also consider regular 1-forms with simple poles away from the nodes: by [Mas76, Proposition 4.2], if p, q are two points on Σ_0 minus the nodes, there exists a unique 1-form $\omega_{p,q,t}$ on Σ_t which has simple poles at p and q with residues 1 and -1, is otherwise regular in the sense above, and has suitably normalized periods (a normalized differential of the third kind). Moreover, $\omega_{p,q,t}$ depends holomorphically on t in a neighborhood of 0.

More specifically, we shall use the following result. For each half-edge $h \in \mathsf{H}$, let A_h denote a small anticlockwise circle in $U_{v(h),\delta}$ around p_h; it is then homologous in Σ_t to a clockwise circle in $U_{v(-h),\delta}$ around p_{-h}.

Proposition 8.1. *Given an antisymmetric function $(\alpha_h)_{h\in\mathsf{H}}$, there exists a unique regular 1-form ω_t on Σ_t, possibly with simple poles at ∞_v, $v \in \mathsf{V}$, such that*

$$\forall h \in \mathsf{H}, \quad \int_{A_h} \omega_t = 2\pi\mathrm{i}\,\alpha_h.$$

Moreover, the restriction of ω_t to U_δ depends holomorphically on t in a neighborhood of 0.

Proof. this follows from [Mas76, Proposition 4.2]. See also [Tra13, Theorem 8.2] for a constructive proof. $\qquad\square$

Note that by the Residue Theorem in $\hat{\mathbb{C}}_v$,

$$\mathrm{Res}\,(\omega_t, \infty_v) = -\sum_{h\in v} \alpha_h.$$

We will also need the following results.

Lemma 8.2 ([Tra08, Lemma 3]). *The derivative $\partial\omega_t/\partial t_h$ at $t = 0$, restricted to U_δ, coincides with a meromorphic 1-form on Σ_0 with double poles at the nodes, holomorphic elsewhere, and vanishing A-periods. In term of the local complex coordinates w_h used to open nodes, the principal part at p_h is*

$$-\frac{d\,w_h}{w_h^2}\,\mathrm{Res}\left(\frac{\omega_0}{w_{-h}}, p_{-h}\right).$$

For every half-edge h and $t_h \neq 0$, let B_h be the concatenation of

(1) a path in $U_{v(h),\delta}$ from $O_{v(h)}$ to $w_h = \delta$,
(2) the path parameterized by $w_h = \delta^{1-2s}\,t_h^s$ for $s \in [0,1]$, from $w_h = \delta$ to $w_h = t_h/\delta$, which is identified with $w_{-h} = \delta$, and
(3) a path in $U_{v(-h),\delta}$ from $w_{-h} = \delta$ to $O_{v(-h)}$.

Lemma 8.3 ([Tra02b, Lemma 1]). *The difference*

$$(9) \qquad\qquad \left(\int_{B_h} \omega_t\right) - \alpha_h \log t_h$$

extends holomorphically to $t_h = 0$. Moreover, its value at $t = 0$ is equal to

$$\lim_{z\to p_h}\left[\left(\int_{O_{v(h)}}^z \omega_0\right) - \alpha_h \log w_h(z)\right] - \lim_{z\to p_{-h}}\left[\left(\int_{O_{v(-h)}}^z \omega_0\right) - \alpha_{-h} \log w_{-h}(z)\right].$$

Lemma 8.3 was essentially proved in [Tra02b, Lemma 1]. As the lemma has been and will be used in similar constructions, we consider it a good time to refurbish the proof in Appendix D.

8.3. **Weierstrass data.** We construct a conformal minimal immersion using the Weierstrass parameterization in the form

$$z \mapsto \operatorname{Re} \int^z (\Phi_1, \Phi_2, \Phi_3),$$

where Φ_i are meromorphic 1-forms on Σ_t satisfying the conformality equation

(10) $$Q := \Phi_1^2 + \Phi_2^2 + \Phi_3^2 = 0.$$

Observe that Q is a meromorphic quadratic differential on Σ_t.

8.3.1. *A-periods.* We need to solve the following A-period problem

$$\operatorname{Re} \int_{A_h} (\Phi_1, \Phi_2, \Phi_3) = (0, 0, 2\pi\sigma_h), \quad \forall h \in \mathsf{H}.$$

We define Φ_1, Φ_2, and Φ_3, using Proposition 8.1, as the unique regular 1-forms on Σ_t with (at most) simple poles at ∞_v for $v \in \mathsf{V}$ and the A-periods

$$\int_{A_h} (\Phi_1, \Phi_2, \Phi_3) = 2\pi\mathrm{i}(\alpha_h, \beta_h, \gamma_h - \mathrm{i}\sigma_h), \quad \forall h \in \mathsf{H},$$

where $(\alpha, \beta, \gamma) \in \mathcal{A}^3$ are antisymmetric parameters. This way, the A-period problems are solved by definition. We choose the following central value for the parameters:

$$\alpha_h^\circ = -\cos(\theta_h^\circ), \qquad \beta_h^\circ = -\sin(\theta_h^\circ), \qquad \gamma_h^\circ = 0.$$

Then at $\varepsilon = 0$ and the central value of all parameters, we have in $\hat{\mathbb{C}}_v$

$$\Phi_1^\circ = \sum_{h \in v} \frac{-\cos(\theta_h^\circ)}{z - p_h^\circ} dz, \quad \Phi_2^\circ = \sum_{h \in v} \frac{-\sin(\theta_h^\circ)}{z - p_h^\circ} dz \quad \text{and} \quad \Phi_3^\circ = \sum_{h \in v} \frac{-\mathrm{i}\sigma_h}{z - p_h^\circ} dz.$$

In other words, $(\Phi_1^\circ, \Phi_2^\circ, \Phi_3^\circ)$ is precisely the Weierstrass data of the saddle tower $\mathscr{S}_v$ as we want.

Note that $\sigma \in \ker(\operatorname{div})$, that is

$$\sum_{h \in v} \sigma_h = 0,$$

so we have by Residue Theorem in $\hat{\mathbb{C}}_v$

$$\operatorname{Res}(\Phi, \infty_v) = -\sum_{h \in v} (\alpha_h, \beta_h, \gamma_h) = -\operatorname{div}_{b(v)}(\alpha, \beta, \gamma).$$

We want ∞_v to be regular points, so we need to solve

(11) $$\operatorname{div}_{b(v)}(\alpha, \beta, \gamma) = \sum_{h \in v} (\alpha_h, \beta_h, \gamma_h) = 0, \qquad \text{for all } v \in \mathsf{V}.$$

If the graph is balanced, then the central values solve (11) at $\varepsilon = 0$. We call (11) the *balance equations*.

Remark 8.4. If we see the surface as a soap film, then the saddle tower at $v(h)$ is pulled by a surface tension force along the wing of h, which can be calculated (up to a physical coefficient) as

$$-\operatorname{Im} \int_{A_h} (\Phi_1, \Phi_2, \Phi_3) = -2\pi(\alpha_h, \beta_h, \gamma_h).$$

8.3.2. *B-periods.* For any cycle $c = (h_1, \cdots, h_n)$ of the graph, let B_c denote the concatenation $B_{h_1} * \cdots * B_{h_n}$ which is a cycle in Σ_t. Recall from Section 3.3.3 the cycle basis $\mathsf{C}^* = \mathsf{F}^* \cup \{c_1, c_2\}$. We need to solve the following B-period problem:

$$(12) \qquad \varepsilon^2 \Big(\operatorname{Re} \int_{B_c} \Phi_1 + \mathrm{i} \operatorname{Re} \int_{B_c} \Phi_2 \Big) = \begin{cases} 0 & c \in \mathsf{F}^*, \\ T_i + \varepsilon^2 \Lambda_i & c = c_i,\ i = 1, 2; \end{cases}$$

$$(13) \qquad \operatorname{Re} \int_{B_c} \Phi_3 = \begin{cases} 0 \pmod{2\pi} & c \in \mathsf{F}^*, \\ \Psi_i \pmod{2\pi} & c = c_i,\ i = 1, 2. \end{cases}$$

8.3.3. *Conformality.* At $\varepsilon = 0$ and the central value of all parameters, Φ_1° has $\deg(v)$ simple poles in $\hat{\mathbb{C}}_v$, hence $\deg(v) - 2$ zeros denoted $\zeta_{v,j}^\circ$ for $1 \leq j \leq \deg(v) - 2$. Recall that these zeros are simple (see the beginning of Section 8). We can also assume that they are not ∞_v. When the parameters are close to their central value, Φ_1 has a simple zero $\zeta_{v,j}$ close to $\zeta_{v,j}^\circ$ in $\hat{\mathbb{C}}_v$ for $1 \leq j \leq \deg(v) - 2$.

Remark 8.5. If the balancing equations are not solved, Φ_1 may have a pole at ∞_v and consequently, an extra zero near ∞_v. We may ignore this zero, as it disappears when the balancing equations are solved. See Proposition 8.6 below.

We will solve the following equations:

$$(14) \qquad \int_{A_h} \frac{Q}{\Phi_1} = 0, \qquad\qquad h \in \mathsf{H},$$

$$(15) \qquad \operatorname{Res}\left(\frac{Q}{\Phi_1}, \zeta_{v,j} \right) = 0, \qquad 1 \leq j \leq \deg(v) - 3,\ v \in \mathsf{V}.$$

Proposition 8.6. *The conformality equation* (10) *is solved if the equations* (11), (14), *and* (15) *are solved.*

Proof. If Equation (11) is solved, then Q and Φ_1 are holomorphic at ∞_v and Φ_1 has no extra zero in $\hat{\mathbb{C}}_v$. By the Residue Theorem in $\hat{\mathbb{C}}_v$

$$\sum_{h \in v} \int_{A_h} \frac{Q}{\Phi_1} + 2\pi\mathrm{i} \sum_{j=1}^{\deg(v)-2} \operatorname{Res}\left(\frac{Q}{\Phi_1}, \zeta_{v,j} \right) = 0.$$

Hence if Equations (14) and (15) are solved, the residue of Q/Φ_1 at the last zero $\zeta_{v,\deg(v)-2}$ must also vanish. So the 1-form Q/Φ_1, being holomorphic on Σ with vanishing A-periods, must be 0. $\qquad\qquad\square$

8.3.4. *Dimension count.* Let us perform a dimension count before proceeding further.

We have $3|\mathsf{E}|$ real parameters (α, β, γ). The complex parameters t comprises $|\mathsf{E}|$ complex numbers. For each $v \in \mathsf{V}$, Möbius transforms on $\hat{\mathbb{C}}_v$ do not change the conformal structure of Σ_t. So we can fix the positions of three of the punctures $(p_h)_{h \in v}$, leaving $\deg(v) - 3$ free complex parameters for each $v \in \mathsf{V}$. So, together with the parameter ε of the family, we have $9|\mathsf{E}| - 6|\mathsf{V}| + 1$ real parameters.

Let us now count the equations. The B-period problems is $3g = 3(|\mathsf{F}| + 1)$ real equations. The conformality equations contain $|\mathsf{E}| + 2|\mathsf{E}| - 3|\mathsf{V}| = 3|\mathsf{F}|$ complex equations. (This is of course the dimension of the space of holomorphic quadratic differentials on Σ_t.) Moreover, we have $3|\mathsf{V}| - 3$ balancing equations (11). Hence there are $9|\mathsf{F}| + 3|\mathsf{V}| = 9|\mathsf{E}| - 6|\mathsf{V}|$ real equations. This is one less than the number of parameters, so 1-parameter families are expected out of our construction.

8.4. **Solving the conformality problem.**

Proposition 8.7. *For $(t, \alpha, \beta, \gamma)$ in a neighborhood of $(0, \alpha^\circ, \beta^\circ, 0)$, there exists $p = (p_h)_{h \in \mathsf{H}}$ depending analytically on $(t, \alpha, \beta, \gamma)$, such that the conformality equations (15) are solved. Moreover, $p_h(0, \alpha^\circ, \beta^\circ, 0) = p_h^\circ$.*

Proof. As in Section 5.4, for each $v \in \mathsf{V}$, we may fix the position of three points p_h in $\hat{\mathbb{C}}_v$ using a Möbius transformation. At $(t, \alpha, \beta, \gamma) = (0, \alpha^\circ, \beta^\circ, 0)$, (Φ_1, Φ_2, Φ_3) restricted to $\hat{\mathbb{C}}_v$ is the Weierstrass data considered in Section 5.4, depending on the parameters $(p_h)_{h \in v}$. By Theorem 5.5, the partial differential of

$$\left(\mathrm{Res}\left(\frac{Q}{\Phi_1}, \zeta_{v,j} \right) \right)_{1 \le j \le \deg(v) - 3}$$

with respect to $(p_h)_{h \in v}$ is an isomorphism. So Proposition 8.7 follows from the Implicit Function Theorem. □

From now on, we assume that p_h are given by Proposition 8.7. We make the change of parameters

$$\alpha_h + \mathrm{i}\beta_h = -\rho_h \exp(\mathrm{i}\theta_h).$$

Clearly, $\rho = (\rho_h)_{h \in \mathsf{H}} \in \mathcal{S}$, and $(\exp(\mathrm{i}\theta_h))_{h \in \mathsf{H}} \in \mathcal{A}^2$. The central values of ρ_h is $\rho_h^\circ = 1$ and the central value of θ_h is θ_h° with $u_h^\circ = e^{\mathrm{i}\theta_h^\circ}$.

Proposition 8.8. *For (t, θ) in a neighborhood of $(0, \theta^\circ)$, there exist unique values of ρ and γ, depending real-analytically on (t, θ), such that the equations (14) are solved. At $t_h = 0$ we have, no matter the values of θ, $(t_k)_{k \ne \pm h}$, and other parameters, that*

$$(16) \qquad \rho_h = 1 \quad and \quad \gamma_h = 0.$$

In particular, we have $|\gamma_h| \le C|t_h|$ for a uniform constant C. Moreover, at $(t, \theta) = (0, \theta^\circ)$, we have the Wirtinger derivatives

$$(17) \qquad \frac{\partial \rho_h}{\partial t_h} = -\frac{1}{2}\Upsilon_h \Upsilon_{-h} \quad and \quad \frac{\partial \gamma_h}{\partial t_h} = -\frac{\mathrm{i}}{2}\sigma_h \Upsilon_h \Upsilon_{-h}.$$

Proof. Define for $h \in \mathsf{H}$

$$\mathcal{E}_h(t, \rho, \gamma, \theta) = \frac{1}{2\pi \mathrm{i}} \int_{A_h} \frac{Q}{\Phi_1}.$$

Assume that $t_h = 0$. Then Φ_1, Φ_2, and Φ_3 have a simple pole at p_h, so Q/Φ_1 has a simple pole at p_h and, by the Residue Theorem

$$\mathcal{E}_h \mid_{t_h = 0} = \frac{\alpha_h^2 + \beta_h^2 + (\gamma_h - \mathrm{i}\sigma_h)^2}{\alpha_h} = \frac{\rho_h^2 + \gamma_h^2 - 1 - 2\mathrm{i}\sigma_h\gamma_h}{\alpha_h}.$$

So the solution of (14) at $t_h = 0$ is $(\rho_h, \gamma_h) = (1, 0)$, no matter the values of the other parameters. This proves (16). We compute the partial derivatives of $\mathcal{E}_h$ with respect to ρ_h and γ_h at $(t, \rho, \gamma, \theta) = (0, 1, 0, \theta^\circ)$:

$$(18) \qquad \frac{\partial \mathcal{E}_h}{\partial \rho_h} = \frac{2}{\alpha_h^\circ}, \qquad \frac{\partial \mathcal{E}_h}{\partial \gamma_h} = \frac{-2\mathrm{i}\sigma_h}{\alpha_h^\circ}.$$

So the existence and uniqueness statement of the proposition follows from the Implicit Function Theorem. To prove the last point, we need to compute the partial derivative of $\mathcal{E}_h$ with respect to t_h at $(t, \rho, \gamma, \theta) = (0, 1, 0, \theta^\circ)$. We use the following elementary results: if $f = a_{-1}z^{-1} + a_0 + O(z)$ and $g = b_{-1}z^{-1} + b_0 + O(z)$ are meromorphic functions with a simple pole at $z = 0$, then

$$\mathrm{Res}\left(\frac{f}{z^2 g}, 0 \right) = \frac{a_0 b_{-1} - a_{-1} b_0}{(b_{-1})^2}, \ \mathrm{Res}\left(f^2, 0 \right) = 2a_{-1}a_0, \text{ and } \mathrm{Res}\left(f^2 z, 0 \right) = (a_{-1})^2.$$

We have

$$\frac{\partial \mathcal{E}_h}{\partial t_h} = \mathrm{Res}\left(\sum_{j=1}^{3} 2\frac{\Phi_j^\circ}{\Phi_1^\circ}\frac{\partial \Phi_j}{\partial t_h}, p_h^\circ\right) \qquad \text{by the Residue Theorem}$$

$$= -2\sum_{j=1}^{3}\mathrm{Res}\left(\frac{\Phi_j^\circ\, dw_h}{\Phi_1^\circ w_h^2}, p_h^\circ\right)\mathrm{Res}\left(\frac{\Phi_j^\circ}{w_{-h}}, p_{-h}^\circ\right) \qquad \text{by Lemma 8.2}$$

$$(19) \qquad = -\frac{2}{\alpha_h^\circ}\sum_{j=1}^{3}\mathrm{Res}\left(\frac{\Phi_j^\circ}{w_h}, p_h^\circ\right)\mathrm{Res}\left(\frac{\Phi_j^\circ}{w_{-h}}, p_{-h}^\circ\right)$$

$$(20) \qquad + \frac{2}{(\alpha_h^\circ)^2}\mathrm{Res}\left(\frac{\Phi_1^\circ}{w_h}, p_h^\circ\right)\sum_{j=1}^{3}\mathrm{Res}\left(\Phi_j^\circ, p_h^\circ\right)\mathrm{Res}\left(\frac{\Phi_j^\circ}{w_{-h}}, p_{-h}^\circ\right).$$

Since $Q^\circ = 0$, we have

$$(21) \qquad \mathrm{Res}\left(\frac{w_h Q^\circ}{dw_h}, p_h^\circ\right) = \sum_{j=1}^{3}\mathrm{Res}\left(\Phi_j^\circ, p_h^\circ\right)^2 = 0,$$

$$(22) \qquad \mathrm{Res}\left(\frac{Q^\circ}{dw_h}, p_h^\circ\right) = 2\sum_{j=1}^{3}\mathrm{Res}\left(\Phi_j^\circ, p_h^\circ\right)\mathrm{Res}\left(\frac{\Phi_j^\circ}{w_h}, p_h^\circ\right) = 0.$$

Because $\mathrm{Res}\left(\Phi_j^\circ, p_{-h}^\circ\right) = -\mathrm{Res}\left(\Phi_j^\circ, p_h^\circ\right)$, Eq. (22) implies that the term (20) vanishes. Note that

$$\frac{1}{\sqrt{2}}\mathrm{Res}\left(\Phi^\circ, p_h^\circ\right), \quad \frac{1}{\sqrt{2}}\mathrm{Res}\left(\overline{\Phi^\circ}, p_h^\circ\right), \quad N^\circ(p_h^\circ)$$

form an orthonormal basis of $\mathbb{C}^3$ for the standard hermitian product $\langle\cdot,\cdot\rangle_{\mathrm{H}}$. After recalling the definition of Υ_h in Section 5.2, we decompose in this basis

$$\mathrm{Res}\left(\frac{\Phi^\circ}{w_h}, p_h^\circ\right) = \frac{1}{2}\left\langle\mathrm{Res}\left(\Phi^\circ, p_h^\circ\right), \mathrm{Res}\left(\frac{\Phi^\circ}{w_h}, p_h^\circ\right)\right\rangle_{\mathrm{H}}\mathrm{Res}\left(\Phi^\circ, p_h^\circ\right) + \sigma_h\Upsilon_h N^\circ(p_h^\circ).$$

Here, the component on $\mathrm{Res}\left(\overline{\Phi^\circ}, p_h^\circ\right)$ vanishes because of (22). In the same way, after recalling that $N^\circ(p_{-h}^\circ) = N^\circ(p_h^\circ)$ and $\sigma_{-h} = -\sigma_h$,

$$\mathrm{Res}\left(\frac{\Phi^\circ}{w_{-h}}, p_{-h}^\circ\right) = \frac{1}{2}\left\langle\mathrm{Res}\left(\Phi^\circ, p_h^\circ\right), \mathrm{Res}\left(\frac{\Phi^\circ}{w_{-h}}, p_{-h}^\circ\right)\right\rangle_{\mathrm{H}}\mathrm{Res}\left(\Phi^\circ, p_h^\circ\right) - \sigma_h\Upsilon_{-h}N^\circ(p_h^\circ).$$

Hence by Equation (19)

$$\frac{\partial \mathcal{E}_h}{\partial t_h} = \frac{-2}{\alpha_h^\circ}\left\langle\overline{\mathrm{Res}\left(\frac{\Phi^\circ}{w_h}, p_h^\circ\right)}, \mathrm{Res}\left(\frac{\Phi^\circ}{w_{-h}}, p_{-h}^\circ\right)\right\rangle_{\mathrm{H}} = \frac{2}{\alpha_h^\circ}\Upsilon_h\Upsilon_{-h}.$$

If $k \neq \pm h$, we have $\partial\mathcal{E}_h/\partial t_k = 0$ as $\partial\Phi_j/\partial t_k$ is holomorphic at p_h°.

We differentiate $\mathcal{E}_h(t, \rho(t,\theta), \gamma(t,\theta), \theta) = 0$ with respect to t_h and obtain, using Equation (18),

$$(23) \qquad \frac{2}{\alpha_h^\circ}\left(\Upsilon_h\Upsilon_{-h} + \frac{\partial\rho_h}{\partial t_h} - \mathrm{i}\sigma_h\frac{\partial\gamma_h}{\partial t_h}\right) = 0.$$

Since $\mathcal{E}_h$ is holomorphic in t_h, we obtain by differentiation with respect to $\overline{t_h}$ and conjugation

$$(24) \qquad \frac{2}{\alpha_h^\circ}\left(\frac{\partial\rho_h}{\partial t_h} + \mathrm{i}\sigma_h\frac{\partial\gamma_h}{\partial t_h}\right) = 0.$$

Solving the system (23), (24) gives Equation (17). □

From now on, we assume that ρ and γ are given by Proposition 8.8.

8.5. **Solving horizontal balance and period problems.** We make the change of parameters

$$t_h = -\exp\left(-\ell_h\varepsilon^{-2} + \mathrm{i}\sigma_h\phi_h\right),\tag{25}$$

where $\ell = (\ell_h)_{h\in\mathsf{H}} \in \mathcal{S}$, and $\phi = (\phi_h)_{h\in\mathsf{H}} \in \mathcal{A}$. The central value of ℓ_h is ℓ_h°, the length of the edge $e(h)$. The central value of ϕ_h is the given phase function ϕ_h°. We combine ℓ and θ into

$$x_h = \ell_h e^{\mathrm{i}\theta_h},$$

whose central value is x_h° as given by the graph.

Proposition 8.9. *Assume that the graph* G *is rigid and balanced. For* (ε, ϕ) *in a neighborhood of* $(0, \phi^\circ)$, *there exist unique values for* $(x_h)_{h\in\mathsf{H}}$, *depending smoothly on* (ε, ϕ), *such that* $x(0, \phi) = x^\circ$ *for all* ϕ *and the horizontal B-period equations* (12) *as well as the* α *and* β *components of the balance equations* (11) *are solved. Moreover,* x *is an even function of* ε *and at* $\varepsilon = 0$, *we have for all* ϕ

$$\frac{\partial^2 x_h}{\partial\varepsilon^2}(0, \phi) = 2\xi_h$$

where ξ_h *is the solution to* (7).

Proof. Define for (ε, x, ϕ) in a neighborhood of $(0, x^\circ, \phi^\circ)$ and $h \in \mathsf{H}$

$$\mathcal{P}_h^{\mathrm{hor}}(\varepsilon, x, \phi) = \varepsilon^2\left(\mathrm{Re}\int_{B_h}\Phi_1 + \mathrm{i}\,\mathrm{Re}\int_{B_h}\Phi_2\right).$$

By Lemma 8.3

$$\lambda_h^{\mathrm{hor}}(\varepsilon, x, \phi) := \left[\left(\mathrm{Re}\int_{B_h}\Phi_1\right) - \alpha_h\log|t_h|\right] + \mathrm{i}\left[\left(\mathrm{Re}\int_{B_h}\Phi_2\right) - \beta_h\log|t_h|\right]$$

extends at $\varepsilon = 0$ to a smooth function of remaining parameters (ε, x, ϕ).

Recall the definition of μ_h in Section 5.2 and that $z_0 = O_v$ is chosen as the origin of the parameterization of the saddle tower $\mathscr{S}_v$. By the last statement of Lemma 8.3, we have at the central value

$$\lambda_h^{\mathrm{hor}}(0, x^\circ, \phi) = \mu_h - \mu_{-h}.$$

We then have

$$\begin{aligned}\mathcal{P}_h^{\mathrm{hor}}(\varepsilon, x, \phi) &= \varepsilon^2\left[(\alpha_h + \mathrm{i}\beta_h)\log|t_h| + \lambda_h^{\mathrm{hor}}(\varepsilon, x, \phi)\right]\\&= -\varepsilon^2\rho_h e^{\mathrm{i}\theta_h}(-\ell_h\varepsilon^{-2}) + \varepsilon^2\lambda_h^{\mathrm{hor}}(\varepsilon, x, \phi)\\&= \rho_h x_h + \varepsilon^2\lambda_h^{\mathrm{hor}}(\varepsilon, x, \phi).\end{aligned}$$

Note that by definition, $\mathcal{P}_h^{\mathrm{hor}}$ is an even function of ε. Since ρ_h is an analytic function of t_h with value 1 at $t_h = 0$ and all derivatives of t_h with respect to ε vanish at $\varepsilon = 0$, we have at $\varepsilon = 0$

$$\mathcal{P}_h^{\mathrm{hor}}(0, x, \phi) = x_h \quad\text{and}\quad \frac{\partial^2\mathcal{P}_h^{\mathrm{hor}}}{\partial\varepsilon^2}(0, x^\circ, \phi) = 2(\mu_h - \mu_{-h}).\tag{26}$$

Now define for c in the cycle basis C^*

$$\mathcal{P}_c^{\mathrm{hor}}(\varepsilon, x, \phi) = \varepsilon^2\left(\mathrm{Re}\int_{B_c}\Phi_1 + \mathrm{i}\,\mathrm{Re}\int_{B_c}\Phi_2\right) = \sum_{h\in c}\mathcal{P}_h^{\mathrm{hor}}(\varepsilon, x, \phi).$$

Then, at $\varepsilon = 0$, we have

$$\mathcal{P}_c^{\mathrm{hor}}(0, x, \phi) = \sum_{h\in c}x_h = P_c^{\mathrm{hor}}(x) \quad\text{and}$$

$$\frac{\partial^2\mathcal{P}_c^{\mathrm{hor}}}{\partial\varepsilon^2}(0, x^\circ, \phi) = 2\sum_{h\in c}(\mu_h - \mu_{-h}) = 2P_c^{\mathrm{hor}}(\mu^a).$$

Regarding the horizontal balance equation (11), we define for b in the cut-basis B^*

$$\mathcal{F}_b^{\mathrm{hor}} = -\operatorname{div}_b(\alpha + \mathrm{i}\beta) = \operatorname{div}_b(\rho_h e^{\mathrm{i}\theta_h}) = \operatorname{div}_b(\rho_h u_h(x)).$$

Again, $\mathcal{F}_b^{\mathrm{hor}}$ is an even function of ε and at $\varepsilon = 0$, we have since $\rho = 1$

$$\mathcal{F}_b^{\mathrm{hor}}(0, x, \phi) = F_b^{\mathrm{hor}}(x) \quad \text{and} \quad \frac{\partial^2 \mathcal{F}_b^{\mathrm{hor}}}{\partial \varepsilon^2}(0, x^\circ, \phi) = 0.$$

We want to solve the system

$$\begin{cases} \mathcal{P}_c^{\mathrm{hor}}(\varepsilon, x, \phi) = 0, & c \in \mathsf{F}^*, \\ \mathcal{P}_{c_i}^{\mathrm{hor}}(\varepsilon, x, \phi) = T_i + \varepsilon^2 \Lambda_i, & i = 1, 2, \\ \mathcal{F}_b^{\mathrm{hor}}(\varepsilon, x, \phi) = 0, & b \in \mathsf{B}^*. \end{cases}$$

If G is balanced, the system is solved at $\varepsilon = 0$ with $x(0, \phi) = x^\circ$ for all ϕ. If G is rigid, then by Implicit Function Theorem, for ε in a neighborhood of 0, there exists a unique solution $x(\varepsilon, \phi)$ depending smoothly on (ε, ϕ) such that $x(0, \phi) = x^\circ$.

Moreover, since the system is even in ε, so is the unique solution $x(\varepsilon, \phi)$. Taking the second derivative of the system with respect to ε at $\varepsilon = 0$ gives

$$\begin{cases} 2 P_c^{\mathrm{hor}}(\mu^a) + P_c^{\mathrm{hor}}\left(\dfrac{\partial^2 x}{\partial \varepsilon^2}(0, \phi)\right) = 0, & c \in \mathsf{F}^*, \\[2mm] 2 P_{c_i}^{\mathrm{hor}}(\mu^a) + P_{c_i}^{\mathrm{hor}}\left(\dfrac{\partial^2 x}{\partial \varepsilon^2}(0, \phi)\right) = 2\Lambda_i, & i = 1, 2, \\[2mm] D F_b^{\mathrm{hor}}(x^\circ) \cdot \dfrac{\partial^2 x}{\partial \varepsilon^2}(0, \phi) = 0, & b \in \mathsf{B}^*. \end{cases}$$

Its unique solution is, by definition, $\frac{\partial^2 x}{\partial \varepsilon^2}(0, \phi) = 2\xi$. $\qquad\qquad\square$

From now on, we assume that the parameters x_h are given by Proposition 8.9.

8.6. Solving vertical balance and period problems.

Proposition 8.10. *Assume that the phase function ϕ° is balanced and rigid. For ε in a neighborhood of 0, there exist unique values for $(\phi_h)_{h \in \mathsf{H}}$, depending smoothly on ε, such that $\phi_h(0) = \phi_h^\circ$ and the vertical B-period problems (13) as well as the γ component of (11) are solved.*

Proof. Similarly to the proof of Proposition 8.9, we define for $h \in \mathsf{H}$

$$\mathcal{P}_h^{\mathrm{ver}}(\varepsilon, \phi) = \operatorname{Re} \int_{B_h} \Phi_3.$$

By Lemma 8.3,

$$\lambda_h^{\mathrm{ver}}(\varepsilon, \phi) := \operatorname{Re}\left[\left(\int_{B_h} \Phi_3\right) - (\gamma_h - \mathrm{i}\sigma_h) \log t_h\right]$$

extends smoothly at $\varepsilon = 0$. By Proposition 8.8, we have $\gamma_h = O(t_h)$ so $\gamma_h \log t_h$ extends smoothly at $\varepsilon = 0$ with value 0. Hence by Lemma 8.3, we have at $\varepsilon = 0$

$$\lambda_h^{\mathrm{ver}}(0, \phi) = \operatorname{Re} \lim_{z \to p_h}\left[\left(\int_{O_{v(h)}}^z \Phi_3^\circ\right) + \mathrm{i}\sigma_h \log w_h(z)\right]$$

$$- \operatorname{Re} \lim_{z \to p_{-h}}\left[\left(\int_{O_{v(-h)}}^z \Phi_3^\circ\right) + \mathrm{i}\sigma_{-h} \log w_{-h}(z)\right]$$

$$= \nu_h - \nu_{-h}$$

where ν_h is defined as in Section 5.2. We then have

$$\mathcal{P}^{\mathrm{ver}}(\varepsilon, \phi) = \lambda_h^{\mathrm{ver}}(\varepsilon, \phi) - \gamma_h \ell_h \varepsilon^{-2} + \phi_h + \sigma_h \pi.$$

Since $\gamma_h = O(t_h)$, we have at $\varepsilon = 0$

$$(27) \qquad \mathcal{P}_h^{\mathrm{ver}}(0, \phi) = \nu_h - \nu_{-h} + \phi_h + \sigma_h \pi.$$

Now define for c in the cycle-basis C^*

$$\mathcal{P}_c^{\mathrm{ver}}(\varepsilon, \phi) = \operatorname{Re} \int_{B_c} \Phi_3 = \sum_{h \in c} \mathcal{P}_h^{\mathrm{hor}}(\varepsilon, \phi).$$

Observe that by Proposition 5.3

$$\sum_{h \in c} (\nu_h - \nu_{-h} + \pi) = \sum_{h \in c} (\nu_h - \nu_{\varsigma(h)} + \pi) = 0 \pmod{2\pi}$$

Hence at $\varepsilon = 0$, we have

$$\mathcal{P}_c^{\mathrm{ver}}(0, \phi) = P_c^{\mathrm{ver}}(\phi) \pmod{2\pi}.$$

Regarding the vertical balance equation (11), we define for b in the cut basis B^*

$$\mathcal{F}_b^{\mathrm{hor}}(\varepsilon, \phi) = -\operatorname{div}_b(\gamma(\varepsilon, \phi)) = -\sum_{h \in b} \gamma_h(\varepsilon, \phi).$$

Using the Mean Value Inequality and Proposition 8.8, we have for $\varepsilon \to 0$

$$\gamma_h(\varepsilon, \phi) = \sigma_h \Upsilon_h \Upsilon_{-h} \operatorname{Im}(t_h(\varepsilon, \phi)) + o(t_h(\varepsilon, \phi)).$$

By Proposition 8.9 and that $\partial x_h / \partial \varepsilon = 0$, we have

$$\frac{\partial^2 x_h}{\partial \varepsilon^2}(0) = \exp(\mathrm{i}\theta_h^\circ) \Big(\frac{\partial^2 \ell_h}{\partial \varepsilon^2}(0) + \mathrm{i}\ell_h \frac{\partial^2 \theta_h}{\partial \varepsilon^2}(0) \Big) = 2\xi_h,$$

so

$$\frac{\partial^2 \ell_h}{\partial \varepsilon^2}(0) = 2 \operatorname{Re}(\xi_h \exp(-\mathrm{i}\theta_h^\circ)).$$

Therefore using Taylor formula

$$\begin{aligned} \operatorname{Im}(t_h(\varepsilon, \phi)) &= -\sigma_h \sin(\phi_h) \exp(-\ell_h(\varepsilon, \phi)\varepsilon^{-2}) \\ &= -\sigma_h \sin(\phi_h) \exp\left(-\ell_h^\circ \varepsilon^{-2} - \operatorname{Re}(\xi_h \exp(-\mathrm{i}\theta_h^\circ)) + O(\varepsilon^2)\right). \end{aligned}$$

Hence we have

$$\mathcal{F}_b^{\mathrm{ver}}(\varepsilon, \phi) = \sum_{h \in b} \Upsilon_h \Upsilon_{-h} \sin(\phi_h) \exp\left(-\ell_h^\circ \varepsilon^{-2} - \operatorname{Re}(\xi_h \exp(-\mathrm{i}\theta_h)) + O(\varepsilon^2)\right).$$

Recall that $\ell_b^\circ = \min\{\ell_h^\circ \mid h \in b\}$ and define for $\varepsilon \neq 0$

$$\widetilde{\mathcal{F}_b^{\mathrm{ver}}}(\varepsilon, \phi) = \exp(\ell_b^\circ \varepsilon^{-2}) \mathcal{F}_b^{\mathrm{ver}}(\varepsilon, \phi).$$

Then $\widetilde{\mathcal{F}^{\mathrm{ver}}}$ extends smoothly at $\varepsilon = 0$ and in the limit $\varepsilon \to 0$ only the shortest edges remain:

$$\widetilde{\mathcal{F}^{\mathrm{ver}}}(0, \phi) = \sum_{h \in m(b)} \Upsilon_h \Upsilon_{-h} \sin(\phi_h) \exp\left(-\operatorname{Re}(\xi_h \exp(-\mathrm{i}\theta_h))\right) = F^{\mathrm{ver}}(\phi).$$

We want to solve the system

$$\begin{cases} \mathcal{P}_c^{\mathrm{ver}}(\varepsilon, \phi) = 0, & c \in \mathsf{F}^*, \\ \mathcal{P}_{c_i}^{\mathrm{ver}}(\varepsilon, \phi) = \Psi_i, & i = 1, 2, \\ \widetilde{\mathcal{F}_b^{\mathrm{ver}}}(\varepsilon, \phi) = 0, & b \in \mathsf{B}^*. \end{cases}$$

If the phase function ϕ° is balanced, the system is solved at $\varepsilon = 0$ by $\phi = \phi^\circ$. If ϕ° is rigid and the cut basis B^* is B_m^* as given by Proposition 3.8, then by the Implicit Function Theorem, the system has a unique solution $\phi(\varepsilon)$, depending smoothly on ε for ε in a neighborhood of 0, such that $\phi(0) = \phi^\circ$. $\qquad \square$

8.7. Geometry and Embeddedness. We have constructed a 1-parameter family of Weierstrass data $(\Phi_{1,\varepsilon}, \Phi_{2,\varepsilon}, \Phi_{3,\varepsilon})$ depending on $\varepsilon > 0$ that solve the Conformality and Period Problems. All parameters are now smooth functions of ε and are denoted accordingly $t_h(\varepsilon)$, $\theta_h(\varepsilon)$, etc... We denote

$$f_\varepsilon = (f_\varepsilon^{\mathrm{hor}}, f_\varepsilon^{\mathrm{ver}}) : \Sigma_{t(\varepsilon)} \to \mathbb{T}_\varepsilon^3$$

the immersion given by Weierstrass Representation formula, decomposed into its horizontal and vertical components. Note that $\Sigma_{t(\varepsilon)}$ and f_ε are independent of the positive number δ used to define Σ_t (although the smaller δ, the smaller ε must be in the definition of Σ_t). We first prove that the immersion is regular, that is:

Proposition 8.11. *we have*

$$(28) \qquad\qquad |\Phi_{1,\varepsilon}|^2 + |\Phi_{2,\varepsilon}|^2 + |\Phi_{3,\varepsilon}|^2 > 0$$

on $\Sigma_{t(\varepsilon)}$ for sufficiently small ε.

Proof. The statement holds in U_δ because the Saddle towers are regular embeddings, and the inequality (28) remains for sufficiently small ε. It suffices to prove (28) on the annuli that we identified to form necks. This is the case if $\Phi_{3,\varepsilon}$ has no zero in the necks.

Recall that Φ_3° has $\deg(v)$ poles hence $\deg(v) - 2$ zeros in $\hat{\mathbb{C}}_v$. By choosing δ sufficiently small, we may assume that all $2|\mathsf{E}| - 2|\mathsf{V}| = 2|\mathsf{F}| = 2g - 2$ zeros lie in U_δ, which remains true for sufficiently small ε. But for $\varepsilon \neq 0$, $\Phi_{3,\varepsilon}$, being a holomorphic function on a Riemann surface of genus g (without nodes), has exactly $2g - 2$ zeros, therefore no other zeros. The statement then follows readily. $\qquad\square$

It remains to prove that the image of f_ε has the desired geometry, as stated in Points (1), (2), (3) of Theorem 6.7, and is embedded. Define

$$X_v(\varepsilon) = f_\varepsilon^{\mathrm{hor}}(O_v).$$

Then $f_\varepsilon - X_v(\varepsilon)$ converges smoothly on $U_{v,\delta}$ to $f_{v,0}$ which parametrize a Saddle tower which we denote $\mathscr{S}_v$. Hence $f_\varepsilon(U_{v,\delta})$ is embedded for $\varepsilon > 0$ small enough. Let $\mathscr{S}_v^\circ$ be the reference saddle tower, namely translated so that the image of O_v is the origin. We denote $\varphi(\mathscr{S})$ the phase of a saddle tower. Using Equation (27) and Proposition 5.3, we have for $h \in \mathsf{H}$

$$\varphi(\mathscr{S}_{v(-h)}) - \varphi(\mathscr{S}_{v(h)}) = \varphi(\mathscr{S}_{v(-h)}^\circ) - \varphi(\mathscr{S}_{v(h)}^\circ) + \lim_{\varepsilon \to 0} \mathcal{P}_h^{\mathrm{ver}}(\varepsilon)$$

$$= \varphi(\mathscr{S}_{v(-h)}^\circ) - \varphi(\mathscr{S}_{v(h)}^\circ) + \phi_h^\circ + \nu_h - \nu_{-h} + \sigma_h \pi$$

$$= \phi_h^\circ \pmod{2\pi}.$$

This proves Point (3). Using Equation (26), we have for $h \in \mathsf{H}$

$$\lim_{\varepsilon \to 0} \varepsilon^2 \left(X_{v(-h)}(\varepsilon) - X_{v(h)}(\varepsilon) \right) = \lim_{\varepsilon \to 0} \mathcal{P}_h^{\mathrm{hor}}(\varepsilon) = x_h^\circ.$$

This proves Point (2). Moreover, because the vertices are represented by distinct points, the images $f_\varepsilon(U_{v,\delta})$ for $v \in \mathsf{V}$ are disjoint for $\varepsilon > 0$ small enough.

For δ and ε small enough, the image of the circle $|w_h| = \delta$ is close to a vertical segment $s_h(\varepsilon)$ lying in $f_\varepsilon(U_{v,\delta})$. On the boundary of the annulus $|t_h|/\delta < |w_h| < \delta$, the gauss map is close to a horizontal constant (from the convergence to saddle towers), so by the maximum principle for holomorphic functions, it is close to this constant on the whole annulus. Given the boundary behavior, the image of this annulus is a graph over a vertical plane, hence embedded. By the convex hull property of minimal surfaces, the image of the annulus $|t_h|/\delta < |w_h| < \delta$ stays close to the vertical plane $B_{e(h)}(\varepsilon)$ bounded by $s_h(\varepsilon)$ and $s_{-h}(\varepsilon)$. After a scaling by ε^2, Point (1) follows.

If there are no parallel edges, by taking $\delta > 0$ small enough, we may ensure that the planes $B_e(\varepsilon)$ for $e \in \mathsf{E}$ are disjoint and conclude that the image of f_ε is embedded because the graph is embedded. The situation is more subtle in the case of parallel edges. Assume that the edges $e(h_1), \cdots, e(h_k)$ are parallel, with $h_1, \cdots, h_k \in v$ and $\varsigma(h_i) = h_{i+1}$ for $1 \leq i \leq k-1$. Because the saddle tower $\mathscr{S}_v$ is embedded, the corresponding ends are asymptotic to parallel but distinct vertical planes. Hence, by our choice of ordering of the ends, the abscissa of the vertical segments $s_{h_i}(\varepsilon)$ are decreasing and separated by a distance greater than some uniform $r > 0$. On the other side, the abscissa of the vertical segments $s_{-h_i}(\varepsilon)$ are also decreasing and uniformly separated. Hence for ε small enough, the planes $B_{e(h_i)}$ for $1 \leq i \leq k$ are disjoint, and we conclude again that the image of f_ε is embedded. This concludes the proof of Theorem 6.7.

Appendix A. Rigidity of saddle towers

This section is dedicated to a proof of Theorem 5.5. Let $\dot{p} \in \ker D\Lambda(p^\circ)$. We want to prove that, if $\dot{p}_h = 0$ for three $h \in \mathsf{H}$, then $\dot{p} = 0$.

Define $p(\epsilon) = p^\circ + \epsilon \dot{p}$. Let $(\Phi_1(\epsilon), \Phi_2(\epsilon), \Phi_3(\epsilon))$ be the Weierstrass data given by Equation (3) and $X(\epsilon)$ the corresponding immersion given by Equation (4). Note that $X(\epsilon)$ is harmonic but not minimal. Let $H(\epsilon)$ be the mean curvature and $N(\epsilon)$ be the normal of $X(\epsilon)$. To ease computation, the dependence on ϵ will not be written. Instead, we use an exponent $\circ$ to denote the value at $\epsilon = 0$ and a dot to denote the partial derivative with respect to ϵ at $\epsilon = 0$.

Lemma A.1. *We have $\dot{H} = 0$ on the Riemann sphere minus the points p_h° for $h \in \mathsf{H}$.*

Proof. We have for all ϵ

$$Q = \sum_{i=1}^{n-2} \lambda_i \frac{\Phi_1 \, dz}{z - \zeta_i} \quad \text{with} \quad \lambda_i = \mathrm{Res}\left(\frac{Q}{\Phi_1}, \zeta_i\right).$$

We have $\lambda_i^\circ = 0$ and $\dot{\lambda}_i = D\Lambda_i(p^\circ) \cdot \dot{p} = 0$ so $\dot{Q} = 0$. Let $w = x_1 + \mathrm{i}x_2$ be a local complex coordinate on the Riemann sphere. Recall the standard formula for the mean curvature

$$(29) \qquad H = \frac{g_{22}b_{11} + g_{11}b_{22} - 2g_{12}b_{12}}{2(g_{11}g_{22} - g_{12}^2)}$$

where g and b are respectively the matrices of the first and second fundamental forms in the coordinate system (x_1, x_2). We have for all ϵ

$$Q = \left(\left\|\frac{\partial X}{\partial x_1}\right\|^2 - \left\|\frac{\partial X}{\partial x_2}\right\|^2 - 2\mathrm{i}\left\langle \frac{\partial X}{\partial x_1}, \frac{\partial X}{\partial x_2}\right\rangle\right) dw^2 = (g_{11} - g_{22} - 2\mathrm{i}g_{12})dw^2.$$

Hence from $Q^\circ = 0$ and $\dot{Q} = 0$ we obtain

$$(30) \qquad g_{11}^\circ = g_{22}^\circ, \quad g_{12}^\circ = 0, \qquad \dot{g}_{11} = \dot{g}_{22} \quad \text{and} \quad \dot{g}_{12} = 0.$$

Since $X(\epsilon)$ is harmonic for all ϵ, we have $b_{11} + b_{22} = 0$ for all ϵ, so

$$b_{11}^\circ + b_{22}^\circ = 0 \quad \text{and} \quad \dot{b}_{11} + \dot{b}_{22} = 0.$$

Taking the derivative of (29), we obtain $\dot{H} = 0$. $\qquad\qquad \square$

By Lemma A.1, $u = \langle \dot{X}, N^\circ \rangle$ is a Jacobi field. In a neighborhood of p_h°, we have

$$(31) \qquad \dot{X} = \mathrm{Re}\left[(\cos(\theta_h), \sin(\theta_h), i\sigma_h)\frac{\dot{p}_h}{z - p_h^\circ}\right] + \text{bounded terms}$$

$$N^\circ = \sigma_h(-\sin(\theta_h), \cos(\theta_h), 0) + O(z - p_h^\circ)$$

so u is a bounded Jacobi field. Since all saddle towers are rigid, there exists $c \in \mathbb{R}^3$ such that $u = \langle N^\circ, c \rangle$. Consider the translated immersion $Y(\epsilon) = X(\epsilon) - \epsilon c$. Then $\langle \dot{Y}, N^\circ \rangle = 0$ so $\dot{Y}$ is a tangent vector. Using the local complex coordinate $w = x_1 + \mathrm{i}x_2$, we decompose $\dot{Y}$ in the tangent space as

$$\dot{Y} = \xi_1 \frac{\partial X^\circ}{\partial x_1} + \xi_2 \frac{\partial X^\circ}{\partial x_2} = \xi \frac{\partial X^\circ}{\partial w} + \bar{\xi} \frac{\partial X^\circ}{\partial \overline{w}} \quad \text{with} \quad \xi = \xi_1 + \mathrm{i}\xi_2.$$

Lemma A.2. $\xi \frac{d}{dw}$ *defines a holomorphic vector field on the Riemann sphere. Moreover,* $\xi(p_h^\circ) = -\dot{p}_h$ *for* $h \in \mathsf{H}$.

Proof. Since X° is conformal and harmonic, we have

$$\left\langle \frac{\partial X^\circ}{\partial w}, \frac{\partial X^\circ}{\partial w} \right\rangle = 0, \qquad \left\langle \frac{\partial X^\circ}{\partial w}, \frac{\partial^2 X^\circ}{\partial w^2} \right\rangle = 0, \qquad \text{and} \quad \frac{\partial^2 X^\circ}{\partial w \partial \overline{w}} = 0$$

where $\langle \cdot, \cdot \rangle$ denotes the $\mathbb{C}$-bilinear dot product. For all ϵ

$$\left\langle \frac{\partial X}{\partial w}, \frac{\partial X}{\partial w} \right\rangle = \frac{1}{4}(g_{11} - g_{22} - 2\mathrm{i}g_{12}).$$

Taking the derivative with respect to ϵ and using Equation (30), we obtain

$$2 \left\langle \frac{\partial X^\circ}{\partial w}, \frac{\partial \dot{Y}}{\partial w} \right\rangle = 2 \left\langle \frac{\partial X^\circ}{\partial w}, \frac{\partial}{\partial w} \left(\xi \frac{\partial X^\circ}{\partial w} + \bar{\xi} \frac{\partial X^\circ}{\partial \overline{w}} \right) \right\rangle = 2 \frac{\partial \bar{\xi}}{\partial w} \left\langle \frac{\partial X^\circ}{\partial w}, \frac{\partial X^\circ}{\partial \overline{w}} \right\rangle = 0.$$

Hence $\frac{\partial \bar{\xi}}{\partial w} = 0$ and ξ is holomorphic. If w' is another local complex coordinate, we can write

$$\dot{Y} = \xi' \frac{\partial X^\circ}{\partial w'} + \overline{\xi'} \frac{\partial X^\circ}{\partial \overline{w'}} = \xi' \frac{\partial X^\circ}{\partial w} \frac{dw}{dw'} + \overline{\xi'} \frac{\partial X^\circ}{\partial \overline{w}} \overline{\left(\frac{dw}{dw'} \right)}$$

This gives

$$\xi = \xi' \frac{dw}{dw'}$$

so ξ transforms as a holomorphic vector field under change of coordinate. Using the complex coordinate $w = z - p_h^\circ$ in a neighborhood of p_h°, we have

$$\frac{\partial X^\circ}{\partial w} = \frac{1}{2w}(-\cos(\theta_h), -\sin(\theta_h), -\mathrm{i}\sigma_h) + O(1).$$

Hence by Equation (31),

$$\xi(p_h^\circ) = -\dot{p}_h.$$

$\square$

Recall that we have fixed the position of three points p_h. Hence ξ has at least three zeros. Now a non-zero holomorphic vector field on the Riemann sphere has two zeros, so $\xi = 0$. This implies that $\dot{p} = 0$ and concludes the proof of Theorem 5.5.

Appendix B. Horizontal rigidity of "triangulated" graphs

This section is dedicated to a proof of Theorem 4.7. Consider, for $x \in \mathcal{H}$, the total length

$$\mathcal{L}(x) = \frac{1}{2} \sum_{h \in \mathsf{H}} \|x_h\|.$$

If $P^{\text{hor}}(\chi) = 0$, so that $\chi = \text{grad} f$, we have

$$\begin{aligned}
D\mathcal{L}(x^\circ) \cdot \chi &= \frac{1}{2} \sum_{h \in \mathsf{H}} \frac{1}{\|x_h^\circ\|} \langle x_h^\circ, f_{v(-h)} - f_{v(h)} \rangle \\
&= -\sum_{h \in \mathsf{H}} \frac{1}{\|x_h^\circ\|} \langle x_h^\circ, f_{v(h)} \rangle \quad (\text{using } h \to -h \text{ for } f_{v(-h)}) \\
&= -\sum_{v \in V} \sum_{h \in b(v)} \frac{1}{\|x_h^\circ\|} \langle x_h^\circ, f_v \rangle \\
&= -\sum_{v \in V} \langle F_{b(v)}^{\text{hor}}, f_v \rangle.
\end{aligned}$$

We have proved that

Proposition B.1. *The graph is balanced if and only if x° is a critical point of $\mathcal{L}$ restricted to those $x \in \mathcal{A}$ such that $P^{hor}(x) = P^{hor}(x^\circ)$.*

Assume that $F^{\text{hor}}(x^\circ) = 0$ and let $\chi = \text{grad}(f)$ be in the kernel of $(DF^{\text{hor}}(x^\circ), P^{\text{hor}})$. Differentiating the above equation

$$D^2\mathcal{L}(x^\circ) \cdot (\chi, \chi) = -\sum_{v \in V} \langle DF_{b(v)}^{\text{hor}}(x^\circ) \cdot \chi, f_v \rangle = 0.$$

On the other hand, a direct computation gives

$$D^2\mathcal{L}(x^\circ) \cdot (\chi, \chi) = \frac{1}{2} \sum_{h \in \mathsf{H}} \frac{1}{\|x^\circ\|^3} \left(\|x_h^\circ\|^2 \|\chi_h\|^2 - \langle x_h^\circ, \chi_h \rangle^2 \right).$$

The summands are all non-negative, hence must be all zero, which means that χ_h is parallel to x_h° for all $h \in \mathsf{H}$.

If all faces have 2 or 3 edges, this implies that $\chi_h = \lambda x_h^\circ$ for some $\lambda \in \mathbb{R}$. Then $P_{c_1}^{\text{hor}}(\chi) = \lambda T_1 = 0$ implies $\lambda = 0$ and $\chi = 0$, which proves Theorem 4.7.

Appendix C. Classification of balanced configurations of genus 3

As promised in Section 7.1, we prove the following Classification Theorem.

Theorem C.1. *The Meeks, aG, aH, and aI configurations in Figure 6 are the only balanced configurations whose graphs are orientable with two faces. Hence they are the only possible configurations that give rise to TPMSs of genus 3.*

Proof. If a configuration gives rise to a TPMS of genus three, its graph must have two faces. By Euler's formula, the average degree of the graph is

$$2|\mathsf{E}|/|\mathsf{V}| = 2(|\mathsf{V}| + |\mathsf{F}|)/|\mathsf{V}| = 2 + 4/|\mathsf{V}|.$$

By Assumption 3.6, the average degree is at least 4, hence the graph has at most 2 vertices. We discuss two cases

$|\mathsf{V}| = 1$, $|\mathsf{E}| = 3$: Then all edges are loops. Since edges are represented by straight segments, no loop is null-homologous. If two loops are homologous, they must be parallel, and represented by the same segment that cuts the torus into an annulus. To form a 2-cell embedding, the remaining edge must be in a different homology class. But then, it is impossible to orient the half-edges alternately incoming and outgoing around the vertex, contradicting the orientability.

So we have three pairwise non-homologous simple loops. They only intersect at the vertex, hence any two of them form a homology basis, and the remaining loop must be homologous to their concatenation. So the graph must be homeomorphic to that of the aH.

Any configuration with this graph is trivially balanced because all edges are loops. It is also trivially rigid as there is only one vertex, so the cut space is trivial.

$|\mathsf{V}| = 2$, $|\mathsf{E}| = 4$: We first prove that such a graph has no loop. The graph is connected, hence the edges can not be all loops. If exactly one or three edges are loops, the degree of a vertex will be smaller than 4, contradicting Assumption 3.6. If exactly two edges are loops, they must be adjacent to different vertices. So they divide the torus into two annuli. Since the graph is represented as a limit of 2-cell embeddings, the remaining edges must lie in different annuli. But then, it is impossible to orient the half-edges alternately incoming and outgoing around each vertex, contradicting the orientability. This proves that none of the edges is a loop.

So we have four edges between two vertices. Any two of the edges form a cycle. If some of these cycles are null-homologous, we will have parallel edges. If at most one edge is simple, it is not possible to form a 2-cell embedding. If exactly two edges are simple, the only 2-cell embedding does not have a proper orientation.

So we have four simple edges between two vertices. Then the graph must be as shown in Figure 11. This graph is balanced if and only if the half-edges form two collinear pairs around each vertex. So if one vertex is at 0, the other vertex must lie at a 2-division point.

By the period condition (6), the phase function must be of the form

$$c - \Psi_2/2, \quad c + \Psi_2/2, \quad c + \Psi_1 + \Psi_2/2, \quad , c + \Psi_1 - \Psi_2/2$$

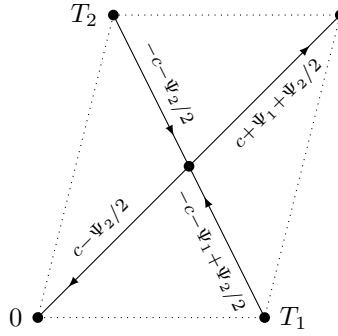on the half-edges around a vertex, where Ψ_1 and Ψ_2 are the fundamental shifts. See Figure 11.

FIGURE 11

If $\arg(T_2/T_1) \neq \pi/2$, the shortest edges of the graph form a collinear pair. Assuming $\arg(T_2/T_1) < \pi/2$ as in Figure 11, then the phase function is balanced if and only if

$$\sin(c + \Psi_1/2) = 0 \quad \text{or} \quad \cos \frac{\Psi_2 - \Psi_1}{2} = 0.$$

The solution $\Psi_1 = -2c$ gives Meeks' configuration which is generically rigid. The solution $\Psi_2 - \Psi_1 = \pi$ gives the aI configurations, which is not rigid because c remains a free variable.

If $\arg(T_2/T_1) = \pi/2$, the phase function is balanced if and only if

$$\sin c + \sin(c + \Psi_1) = 0 \quad \text{or} \quad \cos(\Psi_2/2) = 0.$$

The solution $\Psi_1 = -2c$ gives again Meeks' configurations. The solutions $\Psi_1 = \pi$ and $\Psi_2 = \pi$ give the aG configurations, which is not rigid because c remains a free variable.

$\square$

Appendix D. Integral of a holomorphic 1-form through a neck

To prove Lemma 8.3, we first prove a general result, Theorem D.1 below. This was in fact proved in [Tra02b, Lemma 1] and has been used in several papers, but was not clearly stated as an independent result and the value at $t = 0$ was not explicitly given.

Fix some numbers $0 < \epsilon_1 < \epsilon$. For $t \in \mathbb{C}$ such that $0 < |t| < \epsilon^2$, let $\mathcal{A}_t \subset \mathbb{C}$ be the annulus $|t|/\epsilon < |z| < \epsilon$ and $\psi_t : \mathcal{A}_t \to \mathcal{A}_t$ be the involution defined by $\psi_t(z) = t/z$. Let β_t be the curve from ϵ_1 to t/ϵ_1 parameterized for $s \in [0,1]$ by

$$\beta_t(s) = \epsilon_1^{1-2s} t^s.$$

Note that β_t depends on the choice of the argument of t. Let γ be the circle parameterized by $\gamma(s) = \epsilon_1 e^{2\pi i s}$.

Theorem D.1. *Let ω_t be a family of holomorphic 1-forms on $\mathcal{A}_t$, depending holomorphically on $t \in D^*(0, \epsilon^2)$, and let $\widetilde{\omega}_t = \psi_t^* \omega_t$. Define*

$$\alpha_t = \frac{1}{2\pi i} \int_\gamma \omega_t = -\frac{1}{2\pi i} \int_\gamma \widetilde{\omega}_t.$$

Assume that

$$\lim_{t \to 0} \omega_t = \omega_0 \quad and \quad \lim_{t \to 0} \widetilde{\omega}_t = \widetilde{\omega}_0$$

where ω_0 and $\widetilde{\omega}_0$ are holomorphic in $D^*(0, \epsilon)$ with at most simple poles at $z = 0$, and the limit is uniform on compact subsets of $D^*(0, \epsilon)$.

Then $\int_{\beta_t} \omega_t - \alpha_t \log t$ is a well-defined holomorphic function of $t \neq 0$ which extends holomorphically at $t = 0$. Moreover, its value at $t = 0$ is

$$\lim_{z \to 0} \left[\left(\int_{\epsilon_1}^z \omega_0 \right) - \alpha_0 \log z \right] - \lim_{z \to 0} \left[\left(\int_{\epsilon_1}^z \widetilde{\omega}_0 \right) + \alpha_0 \log z \right].$$

Proof. If $\arg(t)$ is increased by 2π, the homotopy class of β_t is multiplied on the left by γ, so $\int_{\beta_t} \omega_t$ is increased by $2\pi i \alpha_t$. On the other hand, $\log t$ is increased by $2\pi i$, so the difference $\int_{\beta_t} \omega_t - \alpha_t \log t$ is a well-defined holomorphic function of t in $D^*(0, \epsilon^2)$. Using the change of variable rule, we write

$$(32) \quad \left(\int_{\beta_t} \omega_t \right) - \alpha_t \log t = \left[\left(\int_{\epsilon_1}^{\sqrt{t}} \omega_t \right) - \alpha_t \log \sqrt{t} \right] - \left[\left(\int_{\epsilon_1}^{\sqrt{t}} \widetilde{\omega}_t \right) + \alpha_t \log \sqrt{t} \right].$$

To estimate the first term, we fix $\epsilon_1 < \epsilon_2 < \epsilon$ and expand ω_t in Laurent series in the annulus $\mathcal{A}_t$ as

$$\omega_t = \sum_{n \in \mathbb{Z}} a_n(t) z^{n-1} dz$$

with $a_0(t) = \alpha_t$ and

$$a_n(t) = \frac{1}{2\pi i} \int_{|z| = \epsilon_2} z^{-n} \omega_t = \frac{-1}{2\pi i} \int_{|z| = \epsilon_2} \psi_t^*(z^{-n} \omega_t) = \frac{-1}{2\pi i} \int_{|z| = \epsilon_2} t^{-n} z^n \widetilde{\omega}_t.$$

Since ω_t and $\widetilde{\omega}_t$ are uniformly bounded on the circle $|z| = \epsilon_2$, this gives the estimates, for $n > 0$ and a uniform constant C,

$$(33) \quad |a_n(t)| \leq \frac{C}{(\epsilon_2)^n} \quad and \quad |a_{-n}(t)| \leq \frac{C|t|^n}{(\epsilon_2)^n}.$$

Then we have

$$\left(\int_{\epsilon_1}^{\sqrt{t}}\omega_t\right)-\alpha_t\log\sqrt{t}=-\alpha_t\log\epsilon_1+\sum_{n=1}^{\infty}\left[\frac{a_n}{n}\left(t^{n/2}-(\epsilon_1)^n\right)-\frac{a_{-n}}{n}\left(t^{-n/2}-(\epsilon_1)^{-n}\right)\right].$$

Using the estimates (33) and $\epsilon_1 < \epsilon_2$, it is straightforward to check that the sum is uniformly bounded with respect to t and that we have

$$\lim_{t\to0}\left[\left(\int_{\epsilon_1}^{\sqrt{t}}\omega_t\right)-\alpha_t\log\sqrt{t}\right]=-\alpha_0\log\epsilon_1-\sum_{n=1}^{\infty}\frac{a_n(0)}{n}\epsilon_1^n.$$

On the other hand, we have

$$\int_{\epsilon_1}^{z}\omega_0=\alpha_0\log\left(\frac{z}{\epsilon_1}\right)+\sum_{n=1}^{\infty}\frac{a_n(0)}{n}\left(z^n-(\epsilon_1)^n\right)$$

so

$$(34)\qquad\lim_{t\to0}\left[\left(\int_{\epsilon_1}^{\sqrt{t}}\omega_t\right)-\alpha_t\log\sqrt{t}\right]=\lim_{z\to0}\left[\left(\int_{\epsilon_1}^{z}\omega_0\right)-\alpha_0\log z\right].$$

The second term in (32) is estimated in the exact same way, leading to

$$(35)\qquad\lim_{t\to0}\left[\left(\int_{\epsilon_1}^{\sqrt{t}}\widetilde{\omega}_t\right)+\alpha_t\log\sqrt{t}\right]=\lim_{z\to0}\left[\left(\int_{\epsilon_1}^{z}\widetilde{\omega}_0\right)+\alpha_0\log z\right].$$

The function $\int_{\beta_t}\omega_t-\alpha_t\log t$ is bounded so extends holomorphically at $t=0$ by Riemann Extension Theorem. The last point of Theorem D.1 follows from Equations (32), (34) and (35).   □

Proof of Lemma 8.3. Recall the definition of the path B_h just before Lemma 8.3. On path number (1), ω_t depends holomorphically on t_h in a neighborhood of 0 so

$$\int_{O_{v(h)}}^{w_h=\delta}\omega_t$$

is a holomorphic function of t_h in a neighborhood of 0. Same for path number (3). Regarding path number (2) we write

$$(36)\qquad\left(\int_{w_h=\delta}^{w_h=t_h/\delta}\omega_t\right)-\alpha_h\log t_h=\left(\int_{\delta}^{t_h/\delta}(w_h^{-1})^*\omega_t\right)-\alpha_h\log t_h$$

and we apply Theorem D.1 to the 1-form $(w_h^{-1})^*\omega_t$ with $\epsilon_1=\delta$, $t=t_h$, observing that

$$\psi_{t_h}^*(w_h^{-1})^*\omega_t=((\psi_{t_h}\circ w_h)^{-1})^*\omega_t=(w_{-h}^{-1})^*\omega_t$$

so the hypotheses of Theorem D.1 are satisfied. Hence (36) extends holomorphically at $t_h=0$ and its value there is

$$\lim_{z\to0}\left[\left(\int_{\delta}^{z}(w_h^{-1})^*\omega_0\right)-\alpha_h\log z\right]-\lim_{z\to0}\left[\left(\int_{\delta}^{z}(w_{-h}^{-1})^*\omega_0\right)-\alpha_{-h}\log z\right]$$

$$=\lim_{z\to p_h}\left[\left(\int_{w_h=\delta}^{z}\omega_0\right)-\alpha_h\log w_h(z)\right]-\lim_{z\to p_{-h}}\left[\left(\int_{w_{-h}=\delta}^{z}\omega_0\right)-\alpha_{-h}\log w_{-h}(z)\right].$$

Adding the three terms gives Lemma 8.3.

References

[Bra] Ken Brakke. Triply periodic minimal surfaces. `http://facstaff.susqu.edu/brakke/evolver/examples/periodic/periodic.html`.

[Che21] Hao Chen. Existence of the tetragonal and rhombohedral deformation families of the gyroid. *Indiana Univ. Math. J.*, 2021. To appear. 25 pp. Preprint available at `https://www.iumj.indiana.edu/IUMJ/Preprints/8505.pdf`.

[CR01] Claudio Cosín and Antonio Ros. A Plateau problem at infinity for properly immersed minimal surfaces with finite total curvature. *Indiana Univ. Math. J.*, 50(2):847–879, 2001.

[CT21] Hao Chen and Martin Traizet. Stacking Disorder in Periodic Minimal Surfaces. *SIAM J. Math. Anal.*, 53(1):855–887, 2021.

[CW21] Hao Chen and Matthias Weber. An orthorhombic deformation family of Schwarz' H surfaces. *Trans. Amer. Math. Soc.*, 374(3):2057–2078, 2021.

[Die17] Reinhard Diestel. *Graph theory*, volume 173 of *Graduate Texts in Mathematics*. Springer, Berlin, fifth edition, 2017.

[FK87] Werner Fischer and Elke Koch. On 3-periodic minimal surfaces. *Z. Krist.*, 179(1-4):31–52, 1987.

[GGT06] Steven J. Gortler, Craig Gotsman, and Dylan Thurston. Discrete one-forms on meshes and applications to 3D mesh parameterization. *Comput. Aided Geom. Design*, 23(2):83–112, 2006.

[GR01] Chris Godsil and Gordon Royle. *Algebraic graph theory*, volume 207 of *Graduate Texts in Mathematics*. Springer-Verlag, New York, 2001.

[IT94] Alexandr O. Ivanov and Alexei A. Tuzhilin. *Minimal networks*. CRC Press, Boca Raton, FL, 1994. The Steiner problem and its generalizations.

[JS66] Howard Jenkins and James Serrin. The Dirichlet problem for the minimal surface equation, with infinite data. *Bull. Amer. Math. Soc.*, 72:102–106, 1966.

[Kar88] Hermann Karcher. Embedded minimal surfaces derived from Scherk's examples. *Manuscripta Math.*, 62(1):83–114, 1988.

[Kar89] Hermann Karcher. The triply periodic minimal surfaces of Alan Schoen and their constant mean curvature companions. *Manuscripta Math.*, 64(3):291–357, 1989.

[Mas76] Howard Masur. Extension of the Weil-Petersson metric to the boundary of Teichmuller space. *Duke Math. J.*, 43(3):623–635, 1976.

[Mee90] William H. Meeks, III. The theory of triply periodic minimal surfaces. *Indiana Univ. Math. J.*, 39(3):877–936, 1990.

[MRB06] Francisco Martín and Valério Ramos Batista. The embedded singly periodic Scherk-Costa surfaces. *Math. Ann.*, 336(1):155–189, 2006.

[MSSTM18] Shashank G. Markande, Matthias Saba, Gerd Schroeder-Turk, and Elisabetta A. Matsumoto. A chiral family of triply-periodic minimal surfaces derived from the quartz network. 2018. 34 pp. Preprint, `arXiv:1805.07034`.

[MT01] Bojan Mohar and Carsten Thomassen. *Graphs on surfaces*. Johns Hopkins Studies in the Mathematical Sciences. Johns Hopkins University Press, Baltimore, MD, 2001.

[MT12] Filippo Morabito and Martin Traizet. Non-periodic Riemann examples with handles. *Adv. Math.*, 229(1):26–53, 2012.

[PT07] Joaquín Pérez and Martin Traizet. The classification of singly periodic minimal surfaces with genus zero and Scherk-type ends. *Trans. Amer. Math. Soc.*, 359(3):965–990, 2007.

[Sch35] Heinrich F. Scherk. Bemerkungen über die kleinste Fläche innerhalb gegebener Grenzen. *J. Reine Angew. Math.*, 13:185–208, 1835.

[Sch70] Alan H. Schoen. *Infinite periodic minimal surfaces without self-intersections*. National Aeronautics and Space Administration, 1970.

[Tra96] Martin Traizet. Construction de surfaces minimales en recollant des surfaces de Scherk. *Ann. Inst. Fourier (Grenoble)*, 46(5):1385–1442, 1996.

[Tra01] Martin Traizet. Weierstrass representation of some simply-periodic minimal surfaces. *Ann. Global Anal. Geom.*, 20(1):77–101, 2001.

[Tra02a] Martin Traizet. Adding handles to Riemann's minimal surfaces. *J. Inst. Math. Jussieu*, 1(1):145–174, 2002.

[Tra02b] Martin Traizet. An embedded minimal surface with no symmetries. *J. Diff. Geom.*, 60:103–153, 2002.

[Tra08] Martin Traizet. On the genus of triply periodic minimal surfaces. *J. Diff. Geom.*, 79(2):243–275, 2008.

[Tra13] Martin Traizet. Opening infinitely many nodes. *J. Reine Angew. Math.*, 684:165–186, 2013.

[You09]   Rami Younes. *Surfaces minimales dans des variétés homogènes*. PhD thesis, Univer-
             sité de Tours, 2009.

(Chen) Georg-August-Universität Göttingen, Institut für Numerische und Ange-
wandte Mathematik
    Email address: h.chen@math.uni-goettingen.de

(Traizet) Institut Denis Poisson, CNRS UMR 7350, Faculté des Sciences et Techniques,
Université de Tours
    Email address: martin.traizet@univ-tours.fr